EISCAT
TECHNICAL
NOTES

MEASUREMENT PRINCIPLES IN THE EISCAT SYSTEM

by
Hans-Jörgen Alker

KIRUNA
Sweden

EISCAT Technical Note No. 78/5
June 1978

MEASUREMENT PRINCIPLES IN THE EISCAT SYSTEM

by

Hans-Jörgen Alker

This report reproduces the contents of the three first chapters of "A Design Study of a Multibit, Digital Correlator for the EISCAT Radar System", A Thesis by Hans-Jörgen Alker, November 1976.

TABLE OF CONTENTS

CHAPTER 1

INTRODUCTION

During 1974-76 a feasibility study of a digital multibit correlator for the EISCAT (European Incoherent SCATter) system was completed. The main topics for the study were a system-design and hardware selection of a correlator which fulfils the specifications for real-time data-processing in the radar system. This report gives a detailed description of a special-purpose correlator proposed by the author for the EISCAT project.

The EISCAT radar system will be a powerful and comprehensive facility for observing the upper atmosphere in the auroral zone in Scandinavia. The radar observations are based on the scattering of VHF/UHF radio waves caused by thermally-induced irregularities in the plasma. The system will consist of two separate radars: a tristatic UHF system operating at 933.5 ± 5 MHz and a monostatic VHF system at 224 ± 1.5 MHz. Figure 1.1 gives the locations of the transmitting and receiving sites. The UHF-system is fully steerable while the VHF-system is partly steerable (slice along magn. meridian). By measurements involving power- and spectral-analysis of the scattered RF signal, several ionospheric parameters and parameter-variations with altitude may be derived. The RF transmissions by the transmitters will be pulsed in order to obtain range-resolution by time-gating the received signal at the Tromsø site. The range-resolution at the other sites in the UHF system is either given by the intersection of transmitting and receiving antenna beams (long pulse transmissions), or by time-gating the signal. The two radar systems, operating at different frequencies, are necessary for observations over the altitude range from 80 km up to over 2000 km (UHF → 80 km to ∿ 1000 km, VHF → 80 to over 2000 km).

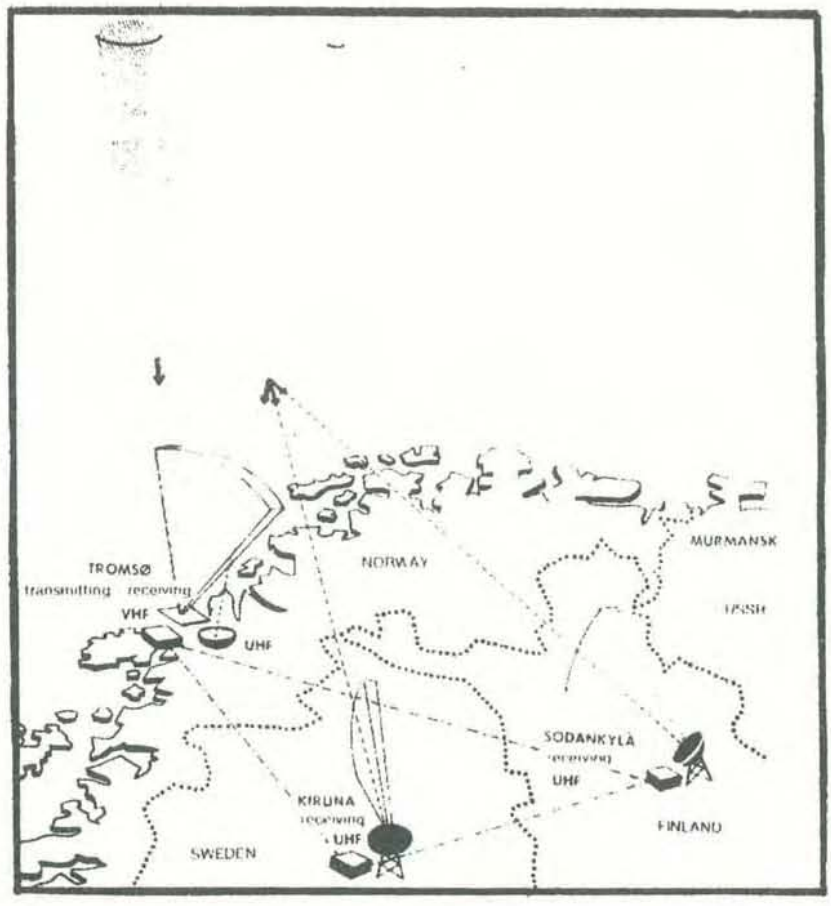

Figure 1.1. Transmitting and receiving locations (from ref.[1])

In the EISCAT system the configuration at each receiver site will be:

- analog, low-noise receivers with separate IF-channels for simultaneously receiving signals from different frequency-bands/polarizations,
- digital programmable correlator for real-time processing,
- analog/digital programmable radarcontroller for real-time control,
- computer for over-all system control, setting of experimental parameters and post-processing of data from the correlator.

In principle, each receiver site can control a complete experiment, with the necessary communication between the computers over data-links.

The incoherent scatter observations in the EISCAT system are based on four principles concerning the data-processing:

- the measurement technique is based on estimating an altitude-dependent autocorrelation function describing the plasma (scattering volume) as a stochastic scattering process,
- the plasma represents for the radar system a weak, deep fluctuating target and in order to obtain statistically accurate estimates relatively long integration times (scan-to-scan integration) are required. For data-reduction purposes real-time high-speed preprocessing of data (correlation function measurements) is necessary,
- parameters defining the real-time computational algorithms are related to the transmitted signal. In order to optimize the measurements, different modulation patterns are to be transmitted, thus requiring the parameters to be programmable and remotely controlled,
- ionospheric parameters are derived by computer post-processing off-line.

Figure 1.2 gives an illustration of the equipment at a receiver site. An experiment is defined by loading a string of "set-up"-parameters from the computer to the radar controller and the correlator. This, in turn, defines the real-time control of the digital correlator, the receiver-system and at Tromsø site the transmitters for performing the experiment. Normally, the on-site computer does not participate in the real-time operations, but acts as a control of the complete system. Pre-processed data are stored in an internal memory of the correlator for the scan-to-scan integration. At pre-determined time-intervals data are transferred to the computer for post-processing (format-conversion, post-integration and tape-recordings.)

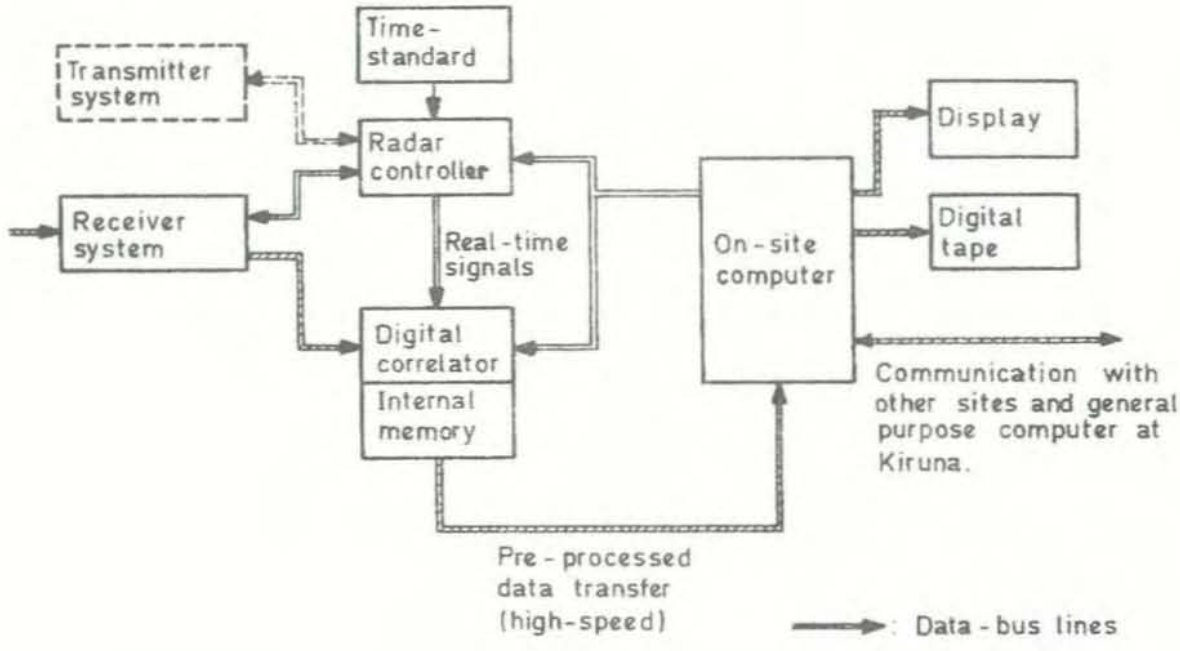

Figure 1.2. EISCAT's receiver site configuration.

The primary purpose of this report is to describe the design and the required hardware of a correlator for the Tromsø site data-processing (monostatic measurements) concerning ion-line measurements. The correlators at the remote sites in the tristatic system have in principle the same operational modes and the hardware realization is close to the proposed solution.

The speed of the on-line computations requires a correlator structure based on a hardware realization with a large degree of internal operations performed in parallel. The proposed realization of the correlator is based on digital components in TTL- and NMOS-technology. These are at present the optimum in relation to power/cost/scale of integration. High-speed arithmetic and control functions are realized using low-power Schottky/Schottky-TTL logic. Internal memory systems are realized in NMOS-technology. The technical hardware solution is in several respects close to the present state of the art. The overall hardware complexity requires that special precautions must be taken for the layout of printed cards and the inter-

connections between subsystems, and also strongly affects reliability and maintenance aspects. A major problem with the chosen TTL-logic is the relatively low noise-margins for the logical levels and the ground-system currents. The total power consumption of the system requires a distributed power-system in order to prevent large current loops. Choosing the optimum digital components has been a problem due to the contemporary rapid development of new components which has made it possible to improve the system with time and reduce costs. For some of the components only preliminary specifications are available. The design of the correlator has followed the ground-rules:

- use of the same hardware for different types of correlation algorithms,
- control and parameters concerning the algorithms can be set remotely by the computer under program control,
- internal hardware control for real-time processing, correlator arithmetic operations in real-time are asynchronous with other parts of the receiver system. A data-buffer between the data acquisition system and the arithmetic modules compensates for the speed mismatch,
- modularity in sub-systems and circuit-layout for test/maintenance purposes. This also permits future hardware improvements by replacing modules.

Although this report describes a special-purpose correlator for the EISCAT system, the report deals with fundamental considerations of equipment for extracting information from radar signals by digital signal processing. Particularly in the fields of pulsed-doppler radars/target-recognition with applications to deep, fluctuating targets, the report should be of general interest in discussing possibilities and limitations of implementing digital hardware for on-line, real-time signal processing.

Scope of the report:

In the following chapter the measurement principles in the EISCAT system are summarized and the required computational algorithms for the correlator are given. In chapter 3 basic types of correlator structures are described and a comparison is made considering the performance. A description of the correlator interfaces with other parts of the receiver system may be found in chapter 4. Design specifications for the correlator are covered in chapter 5, where the choice of basic parameters is discussed. Chapter 6 deals with the operating principles of the proposed system. Chapter 7 gives a general view of the organization of the hardware modules, card interconnections and required bus-lines. This chapter also describes the concept chosen for the power distribution. Chapter 8 provides a cost estimate of the involved hardware. Chapter 9 gives a present report on the realization of correlator modules. In the conclusion, chapter 10, a comparison is made with other existing correlators for this application.

A detailed description of the correlator hardware modules is given in appendix C (separate volume).

Chapter 2

MEASUREMENT PRINCIPLES IN THE EISCAT SYSTEM

The theory of the scattering of VHF/UHF radio waves by a plasma is well understood. The scattering process represented by the ionosphere is best visualized as caused by density fluctuations. These fluctuations are random and resulting from the thermal motions of the particles. The scattered signal is noise-like and its spectrum is Doppler-broadened due to the time variation in the medium. The name incoherent scatter has been given to the process because the average scattered power is propotional to the density. By estimation of the "Doppler-spectrum", plasma characteristics are derived. A summary of theoretical works, experimental techniques and results obtained at existing radar facilities can be found in ref. [2] - [4].

The EISCAT radar system will operate at frequencies which are essentially higher than the plasma frequency of the ionosphere along the transmission path. At these frequencies the scattering is weak. The observed backscattered signal is caused by electron density fluctuations of scale λ_p which for backscatter is:

$$\lambda_p = \frac{\lambda_T}{2} \qquad \lambda_T\text{: radar wavelength}$$

For the EISCAT system:

$$\lambda_p = 66.9 \text{ cm VHF}$$

$$\lambda_p = 16.1 \text{ cm UHF}$$

The electron density fluctuations at the given scale are controlled by the positively charged ions in the ionosphere, provided λ_p is much larger than the Debye- length h_D of the plasma. In fact, the spectrum of the scattered signal may be split into two parts: the ion component which is the portion with Doppler- shifts corresponding to the ion thermal velocities (centered approximately at the radar frequency),

and the electronic component which appears as "spectral lines" displaced from the centre frequency at either side by approximately the plasma frequency when $\lambda_p >> h_D$. When $\lambda_p << h_D$ the ion component disappears and instead of the spectral lines the electronic component appears as a broad Gaussian spectrum corresponding to the electron thermal motions. The bandwidth defined by the spectral lines is typically 20 MHz. The primary purpose of this report is to design a correlator for the estimation of the center part of the backscatter spectrum, the ionic component, which has a bandwidth of typically 10 kHz (VHF) or 30 kHz (UHF). This design-philosophy limits the correlator performance in that it excludes the plasma line observations. It has been chosen to limit the system/hardware complexity for ion component measurements. By choice of a flexible hardware concept we have tried to incorporate some of the plasma-line requirements in the design.

The radar observations are based on measuring four basic parameters of the received radar IF-signals: (1) power, (2) complex auto/cross correlation functions, (3) (VHF-system only) the polarization (Faraday rotation) and (4) the frequencies and shapes of the up-and down-shifted plasma line. The parameters are to be estimated as a function of altitude with a desired altitude-resolution. The incoherent-scatter signal to be detected is embedded in background and receiver noise. The estimation of ionspheric parameters with sufficient accuracy must be performed after a proper correction for noise and systematic effects. For monostatic measurements the period between transmission of pulses is divided into time-intervals (range-gates) corresponding to the range-resolution. It is required that spectral analysis is performed for each range-gate. As indicated, the signal processing is based on estimating correlation functions. Using a digital correlator instead of traditional filter-bank processing is convenient for incoherent-scatter observations, the main advantages being the strict hardware stability and the flexibility of adapting the device.

In the EISCAT system a variety of different transmitted waveforms are to be used in order to optimize the extraction of the plasma autocorrelation function under the constraints given by the plasma (ionosphere) itself and the transmitter/receiver characteristics. By referring to appendix A where a simplified mathematical model for monostatic observations is derived, the next sections discuss fundamental aspects of the measuring method and give the necessary arithmetic algorithms for the correlator.

2.1. THE PLASMA AUTOCORRELATION FUNCTION

By applying a one-dimensional model for describing monostatic observations, the stochastic scattering process can be characterized by a three-dimensional complex autocorrelation function:

$$R_M(\tau, h, 2k_T) \tag{2.1}$$

the variables range in timelag τ, altitude h and wavenumber k_T, the wavenumber of the incident wave.

$$k_T = \frac{2\pi f_T}{c}$$

where f_T: transmitter frequency, c: velocity of light. $2k_T$ is a parameter defining the scale of the observations. The variations of the observed autocorrelation function with k_T can be explained by the fact that the transmitted signal acts as a Fourier analyzer of the medium, picking out the component of the spatial fluctuation spectrum which has the correct scale for backscattering.

The plasma autocorrelation function R_M or its Fouriertransform can be computed theoretically (ref. [2]) using a model ionosphere. In table II.1. typical bandwidths of the ion component of the fluctuation spectrum are computed. The computations are performed for the model ionosphere given in table 2.3.1.

in ref. [5]. For the half-power width is used:

$$B = 1.6 \cdot 2\Delta f_i$$

$$2\Delta f_i = \frac{4}{\lambda_T}\sqrt{\frac{2kT_i}{m_i}} \quad \text{Hz} \tag{2.2}$$

λ_T : radar wavelength
k : Boltzmann's constant
T_i : the ion temperature
m_i : the ion mass

The parameter $\tau_M = \frac{1}{B}$ gives approximately the first zero crossing of the autocorrelation function. The table also gives the desirable range-resolution for measurements under average conditions (table 3.3.1. in ref. [5]).

VHF (λ_T = 1.34 m):

Altitude (km)	85	100	120	200	500	1000	2000
Bandwidth B (kHz)	1.57	1.75	1.92	3.65	5.23	8.20	10.68
Corr.time τ_M (μsec)	637	571	521	274	191	123	94

UHF (λ_T = 32.1 cm):

Altitude (km)	85	100	120	200	500	1000
Bandwidth B (kHz)	6.53	7.30	7.99	15.20	21.79	34.18
Corr.time τ_M (μsec)	153	137	125	66	46	29

VHF/UHF :

Altitude range (km)	85-100	100-120	120-220	220-500	500-1000	1000-2000
Altitude resolution (km)	1	2	15	15	75	150

Table II. 1. Typical bandwidths/correlation-times for ion component.

Desirable range-resolutions under average conditions.

2.2. TYPICAL MODULATION MODES. CONSTRAINTS GIVEN BY THE TRANSMITTER/RECEIVER SYSTEM.

In appendix A it is shown that the autocorrelation function of the backscattered signal (complex amplitude v_o) at the receiver output is related to the plasma autocorrelation function R_M through:

$$R_o(\tau,t) \triangleq E\left[v_o^*(t-\tfrac{\tau}{2}) v_o(t+\tfrac{\tau}{2}) \right]$$

$$= \int_h \int_\lambda R_M(\tau-\lambda,h,2k_{To}) \cdot K(\tau,\lambda,h,t)\,d\lambda\,dh \qquad (2.3)$$

h: altitude
τ,λ : lag-parameters
$E[\cdot]$: ensemble average
* : complex conjugate

The function K is defined by:

$$K(\tau,\lambda,h,t) \triangleq \int_\theta v_T^*(t-\theta-\tfrac{\tau}{2}-\tfrac{2h}{c}) v_T(t-\theta-\lambda+\tfrac{\tau}{2}-\tfrac{2h}{c}) \qquad (2.4)$$

$$\times\, h^*_{R,LP}(\theta) h_{R,LP}(\theta+\lambda)\,d\theta$$

v_T: complex amplitude of transmitted signal.

$h_{R,LP}$: complex amplitude of receiver-system's impulseresponse.

To a first approximation the variations of R_M with k_T in eq. 2.3 are neglected. The parameter k_{To} is given by:

$$k_{To} = \frac{2\pi f_0}{c} \qquad f_0: \text{ radar centre frequency.} \qquad (2.5)$$

The integrals over h and λ in eq. 2.3 express the altitude and lag smearing of the plasma autocorrelation function. The weight-function K is determined by the transmitted signal/ receiver-system.

By the assumption that R_M is constant over the altitude interval and t fixed:

$$R_o(\tau;t) = \int_{\lambda} R_M(\tau-\lambda, h = \frac{ct}{2}, 2k_{To}) \cdot R_T(\tau-\lambda;t) \cdot R_R(\lambda)\,d\lambda \tag{2.6}$$

$$= \left[R_M \times R_T\right] \ast R_R \qquad \ast: \text{convolution}$$

$$R_T(\tau-\lambda;t) \triangleq \int_{h} v_T^*(t-\theta-\frac{\tau}{2}-\frac{2h}{c}) v_T(t-\theta-\lambda+\frac{\tau}{2}-\frac{2h}{c})\,dh \tag{2.7}$$

$$R_R(\lambda) \triangleq \int_{\theta} h_{R,LP}^*(\theta) h_{R,LP}(\theta+\lambda)\,d\theta \tag{2.8}$$

Equation 2.6 states that the autocorrelation function of the backscattered signal at the receiver output is generated by linear operations on R_M. The functions R_T and R_R are in principle deterministic, thus implying that the systematic effects caused by the transmitted signal and receiver system characteristics can to some extent be corrected. Another implication is that the weight-function K in eq. 2.3 can be chosen by a proper signal- and receiver-system design to possess optimum properties for the extraction of the plasma autocorrelation function.

A basic limitation on the extraction of the plasma autocorrelation function exists due to the pulsed transmissions of the radar system for monostatic observations. Assuming that the receiver system has minor effects on the backscattered signal in the frequency band given by the transmitted spectrum convolved with the ion component of the plasma fluctuation spectrum, equation 2.3 can be rewritten:

$$R_o(\tau;t) \sim \int_h R_M(\tau,h,2k_{To}) v_T^*(t-\frac{\tau}{2}-\frac{2h}{c}) v_T(t+\frac{\tau}{2}-\frac{2h}{c}) dh \qquad (2.9)$$

R_M: ionic part.

In case the transmitted signal has a time-duration τ_T, it follows that:

$$v_T^*(t-\frac{\tau}{2}-\frac{2h}{c}) v_T(t+\frac{\tau}{2}-\frac{2h}{c}) \equiv 0 \quad \text{for } \tau > \tau_T \qquad (2.10)$$

This implies that only a truncated plasma autocorrelation function can be extracted, the width of the observational window being determined by the pulse-length τ_T of the transmitted signal. Assuming that R_M varies slowly over the actual h:

$$R_o(\tau;t) \sim R_M(\tau, h = \frac{ct}{2}, 2k_{To}) \cdot R_T(\tau;t) \qquad (2.11)$$

The truncation of the autocorrelation function causes, in terms of spectral resolution, a smoothing of the true plasma fluctuation spectrum. Assuming that the plasma autocorrelation function can be recontructed inside a rectangular window extending over $-\tau_T < \tau < \tau_T$, the plasma spectrum is convolved with the spectrum:

$$2\tau_T \frac{\sin 2\pi f \tau_T}{2\pi f \tau_T} \qquad (2.12)$$

Defining the frequency-resolution by the centre lobe:

$$\Delta f = \frac{1}{\tau_T} \qquad (2.13)$$

it follows that spectral resolution is inverse proportional to the time duration of the transmitted signal. The altitude-resolution is given by the integral over h in eq. 2.9, the altitude weight-function being defined by:

$$W_T(\tau,h;t) \triangleq v_T^*(t-\frac{\tau}{2}-\frac{2h}{c})\ v_T(t+\frac{\tau}{2}-\frac{2h}{c}) \qquad (2.14)$$

In the following subsections typical modulation modes to be used in the EISCAT system are presented.

2.2.1. SINGLE-PULSE MODE

The complex amplitude of the transmitted waveform can be expressed as:

$$v_T(t) = \begin{cases} \sqrt{2P_T}\ e^{j\varphi} & \text{for } |t| \leq \tau_T \\ 0 & \text{else} \end{cases} \qquad (2.15)$$

P_T: peak power
τ_T: time-duration of pulse

Figure 2.1 gives a sketch of the weight-function W_T for t and τ fixed and the autocorrelation function R_T. The altitude-resolution decreases with increasing lagparameter τ and the maximum obtainable lag for the truncated R_M is given by the pulse-length τ_T.

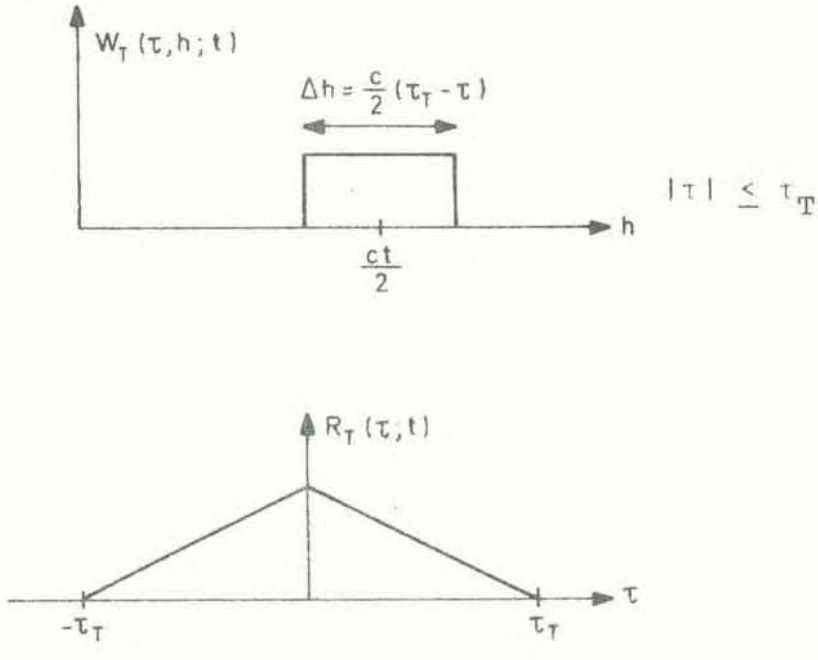

Figure 2.1. Altitude weight-function and autocorrelation function of the transmitted signal for single-pulse transmissions. Receiver-system effects have been neglected.

Observations using single-pulse transmissions can be divided into two classes:

- electron-density profile measurements implying that backscattered power is estimated as a function of altitude, i.e. $R_M(o,h,2k_{To})$ is determined as a function of h.
- "spectral" information measurements, i.e. $R_M(\tau,h,2k_{To})$ as a function of τ and h.

For the latter a trade-off between simultaneous frequency- and altitude-resolution exists. Spectral observations require that the plasma autocorrelation function should be estimated for lag-intervals corresponding to $2\tau_M$-$5\tau_M$, the parameter τ_M being the first zero crossing of R_M. Due to the degradation effect of the multiplication with R_T, the autocorrelation analysis of the received signal can be made up to a maximum lag about $\frac{\tau_T}{2}$ (ref.[6]). This states that the typical pulse-lengths of the transmitted signal are:

$$\tau_T \rightarrow 2\tau_M\text{-}10\tau_M. \qquad (2.16)$$

For the lower bound it is assumed that the maximum lag is of the order of the transmitted pulse-length.

Table II.2 gives a comparison of requirements for the transmitted pulse-length on the basis:

- pulse-length for satisfying the desirable range-resolution (table II.1):

$$\tau_T = \frac{2\Delta h}{c}$$

- pulse-length for satisfying spectral resolution requirements (using the lower bound in eq. 2.16):

$$\tau_T = 2\tau_M$$

In the table typical bandwidth requirements are also given for the receiver-system. The bandwidth of the backscattered signal at the receiver input is determined by the convolution of the plasma spectrum with the spectrum of the transmitted signal. A simplified expression for the receiver bandwidth is:

$$B_R \sim B_T + B \approx \frac{2}{\tau_T} + B \qquad (2.17)$$

B_T: spectrum of trans. signal

B : plasma spectrum

τ_T: pulse-length meeting the range-resolution requirements

Altitude range	85-100	100-120	120-220	220-500	500-1000	1000-2000
Desirable range resolution (km)	1	2	15	15	75	150
1) Required pulse-length for the range resolution (μsec)	6.7	13.3	100	100	500	1000
2) Required pulse-length for spectral observations (μsec) UHF-system	306-250	274-250	250-132	132-92	92-58	
2) Required pulse-length for spectral observations (μsec) VHF-system	1274-1142	1142-1042	1042-548	548-382	382-246	246-188
Receiver bandwidth UHF-system (kHz)				35-42	26-38	
Receiver bandwidth VHF-system (kHz)					9-12	10-13

Table II.2. Single-pulse mode. Comparison of requirements on transmitted pulse-length for satisfying:

1) desirable range-resolution

2) estimating the autocorrelation function of the ion component for lags up to two times the first zero crossing.

Bandwidth of receiver-system for altitude regions where the single-pulse mode can be used for spectral observations.

Values computed are valid for average conditions.

From the table it follows that single-pulse transmissions are limited to high altitude spectral observations (F-region measurements).

For electron-density profile measurements the single-pulse mode can be applied for the complete altitude range with pulse-lenghts τ_T meeting the specification for range-resolution. Whenever $\tau_T < \tau_M$ pulse-compression techniques can be applied (ref. [7]) either to enhance the sensitivity or increase the range-resolution. In the EISCAT system matched-filter design for Barker-codes has been considered. In figure 2.2 the transmitted envelope for a 13-baud Barker code and the weight-function $K(\tau,\lambda,h,t+\tau_T)$ in eq. 2.4 for $\tau,\lambda = 0$ are plotted. The centre peak is proportional to the energy of the transmitted pulse while the range-resolution (half-value width) is given by

$$\Delta h = \frac{c\tau_b}{2} \tag{2.18}$$

where τ_b is the baud-length. The side-lobe level is $\frac{1}{13}$ of the centre peak.

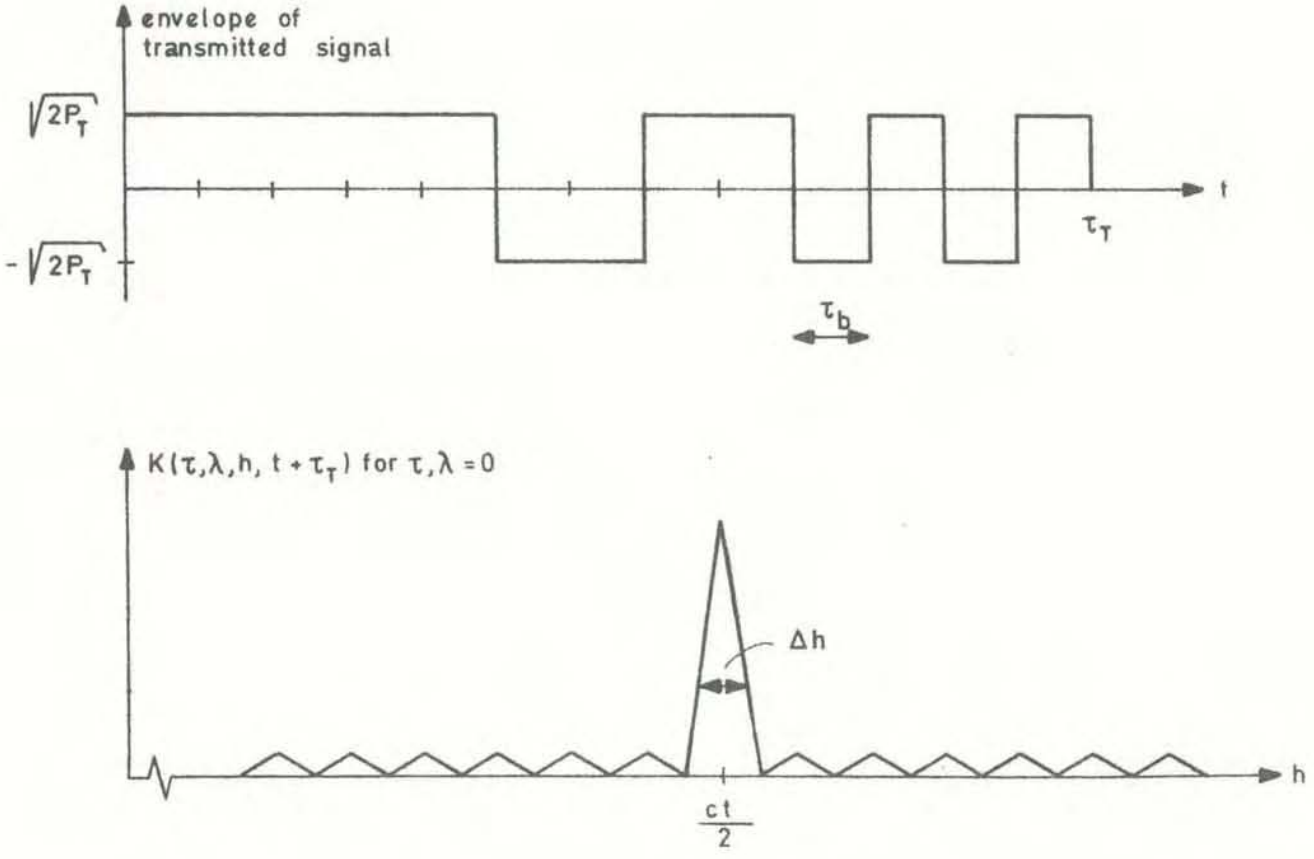

Figure 2.2. 13-baud Barker code and corresponding altitude weightfunction K (eq. 2.4) for $\tau,\lambda = 0$

Transmitter system considerations:

Basic parameters for the UHF/VHF transmitters are given in appendix B. In order to make full use of the radar duty cycle it is possible to perform centre-frequency hop. The EISCAT UHF-receiver will have 8 separate IF channels for receiving backscattered signals at the different centre-frequencies (REF. [8]). Provided the frequency hop is larger than the received signal bandwidth the signals at the receiver outputs are statistically independent. By this technique the number of independent data-samples per sec can be increased. The constraints of the transmitter system can be explained by the following example:

Assuming the autocorrelation function to be estimated in the altitude interval 750-1000 km at UHF with a range-resolution of 75 km, the transmitted pulse length is 0.5 msec. The delay-time corresponding to the given interval equals 5-6.7 msec. In order to perform background noise estimation and prevent range ambiguity the pulse repetition period T is about 12 msec (1800 km). The duty cycle is then

$$DC_{\text{single-pulse}} \triangleq \frac{\tau_T}{T} = 4.17\%$$

The duty cycle for the UHF system is limited to 12.5%, thus implying that a transmitted waveform of duration $3 \cdot \tau_T$ should be transmitted, τ_T at 3 different centre frequencies, without changing the period time T. Increasing the number of frequencies beyond 3 is wastfulbecause the number of data-samples pr. sec. will not increase provided the peak power is kept constant. This can be explained by the following:

Assuming the number of data-samples from one IF channel in a single interpulse period is n, the number of samples pr. sec. is n/T. The total number of samples pr. sec. is $k \cdot n/T$, where k is the number of frequencies. Assuming now that the duty cycle requirement is fulfilled.

$$\frac{P_T \; k \; \tau_T}{T} = P_M$$

P_T: peak power $_{MAX}$

P_M: average power $_{MAX}$

it follows that

$$\frac{kn}{T} = \frac{n}{\tau_T} \cdot \frac{P_M}{P_T}$$

which is independent of k. The improvement-factor for the number of samples pr. sec. is

$$\frac{P_M}{P_T} \cdot \frac{T}{\tau_T} = \frac{DC_{MAX}}{DC_{\text{single pulse}}} \qquad (2.19)$$

which for the example is 3 and can be attained by 3 frequencies.

2.2.2. MULTIPLE-PULSE MODE

In equation 2.11 the autocorrelation function of the back-scattered signal is given by $R_M \times R_T$. This multiplicative property can be used to perform a "sampling" of the plasma autocorrelation function R_M by constructing a transmitted waveform with an autocorrelation function which has "peaks" for the desirable lag-parameters. Assuming that a waveform can be constructed with limited altitude contributions for the specific lags, the trade-off between simultaneous altitude - and frequency-resolution can be avoided. The sampling is possible by transmitting a sequence of short pulses and choosing the pulse positions such that each "peak" in the autocorrelation function receives contributions only from two element pulses. The altitude resolution is then determined by the length of the element pulse through:

$$\Delta h = \frac{c\tau_e}{2} \qquad (2.20)$$

τ_e: time-duration of element pulse.

The maximum lag obtainable on R_M is given by the time delay between the first and last pulse in the sequence. In figure 2.3 a four-pulse group is sketched. The plasma autocorrelation function can be estimated for lags equal to all time delays

between the pulses. In the multiple-pulse mode the bandwidth of the transmitted signal is large compared with the ion component of the plasma spectrum, and the optimum filter-design for the receiver system is the matched filter for the element pulse. The resulting weight-function $K(\tau,\lambda,h,t),\lambda = 0$ in eq. 2.4 is sketched in figure 2.4 for the given lags. Provided the element pulse length $\tau_e \leq \frac{\tau_1}{2}$ where τ_1 is the smallest lag the weight-function will have no sidelobes which could give correlated clutter from other pulses in the group.

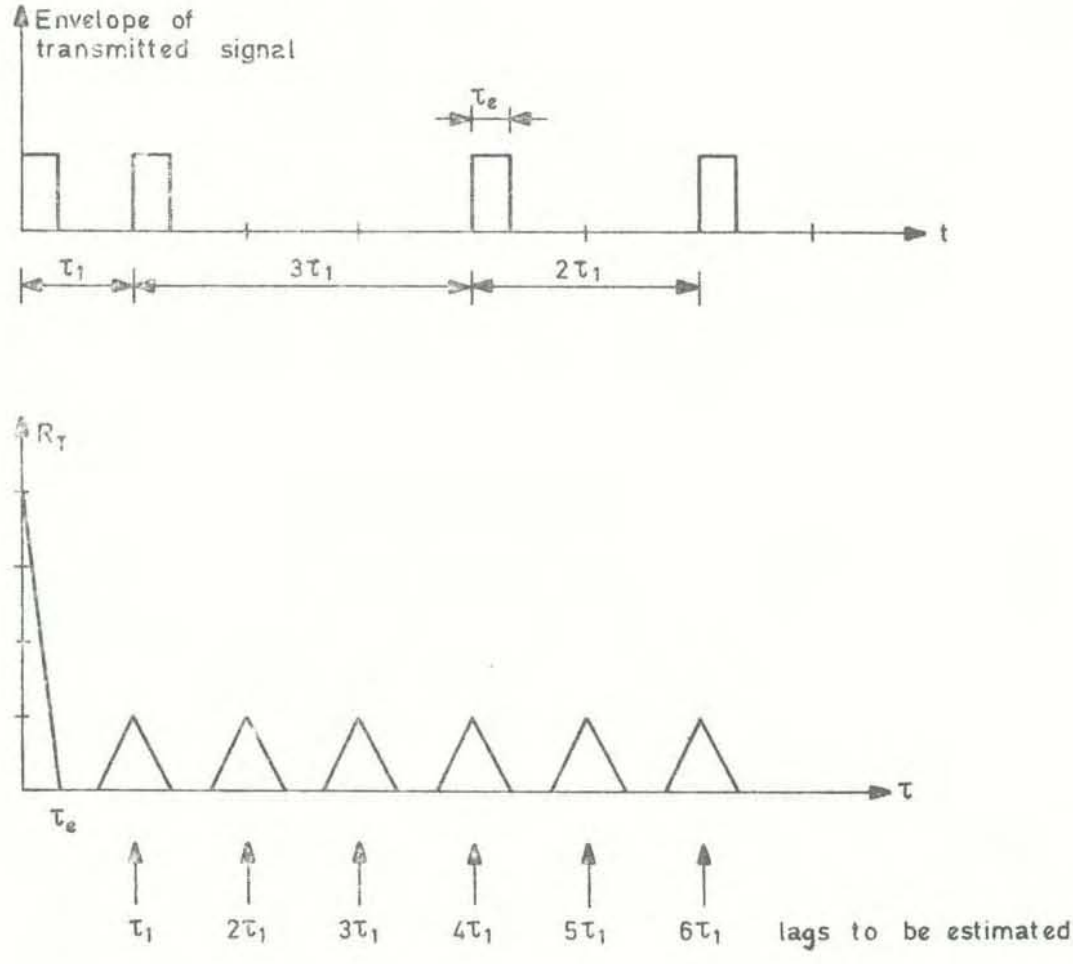

Figure 2.3. Multiple-pulse mode. Four-pulse group

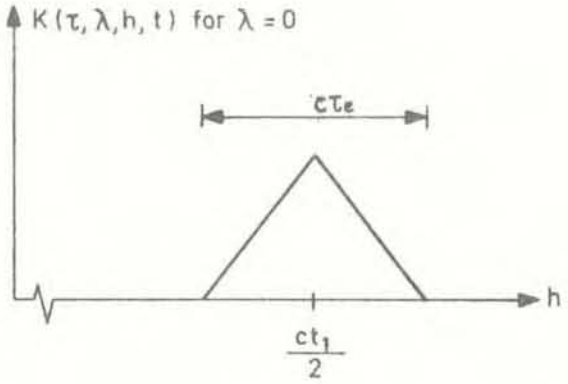

lags:	time:
$\tau=\tau_1$	$t=t_1+\tau_e+\frac{\tau_1}{2}$
$\tau=2\tau_1$	$t=t_1+\tau_e+5\tau_1$
$\tau=3\tau_1$	$t=t_1+\tau_e+\frac{5}{2}\tau_1$
$\tau=4\tau_1$	$t=t_1+\tau_e+2\tau_1$
$\tau=5\tau_1$	$t=t_1+\tau_e+\frac{7}{2}\tau_1$
$\tau=6\tau_1$	$t=t_1+\tau_e+3\tau_1$

Figure 2.4. Weight-function K(eq. 2.4) for $\lambda = 0$.
Multiple-pulse transmissions.

In ref. [8] pulse-groups from 2 to 7 pulses are given. In the EISCAT system 2-10 pulses can be applied. Assuming a number of pulses n_p, the total number of lags is given by $n_p(n_p-1)/2$. The zero lag estimate (power estimate) is not obtainable because of the range ambiguity. The multiple-pulse group is to be transmitted at the same centre frequency. Characteristic of this modulation mode is the "self"-noise contributions from pulses other than the one at the desirable altitude. In a situation where this clutter is dominant compared with system - and background-noise, an increase of peak-power will not increase the sensitivity. This implies that additional power, if available, should be distributed to pulse-groups transmitted at different frequencies. For the VHF-system change in polarization is possible (right/left circular polarization), which applied to a two pulse experiment will eliminate the self-noise contributions. In this case a cross-correlation of signals from two separate receiver systems must be performed. For a multiple-pulse experiment each element pulse can be phase-coded. In ref. [6] a minimum baud-length of 2 μsec was considered for the EISCAT UHF-system, giving an altitude-resolution of the order of:

$$\Delta h_{MIN} \sim 300 \text{ meters} \qquad (2.21)$$

for monostatic observations.

The multiple-pulse mode is to be applied to low altitude observations (D and E regions), but can, in principle, be used for the complete altitude interval provided an increased altitude-resolution is required.

2.2.3. FARADAY ROTATION EXPERIMENTS

The incoherent scatter technique can be used for extracting Faraday rotation angle information (ref. [9]). These observations are based on estimating the relative phase of the left- and right-circularly polarized signals backscattered from the ionosphere as a function of altitude. The phase-information is estimated by crosscorrelation of signals received in separate receivers for the two polarization modes, and will give an alternative method for the determination of the electron-density. This type of measuring method can only be performed by the VHF system.

2.3. ESTIMATION OF CORRELATION FUNCTIONS. REQUIRED ARITHMETIC ALGORITHMS.

The extraction of the plasma autocorrelation function or the polarization angle is based on the determination of the ensemble average:

$$R_o(\tau,t) \triangleq E\left[v_o^*(t-\tfrac{\tau}{2})w_o(t+\tfrac{\tau}{2})\right] \qquad (2.22)$$

where v_o, w_o, are observed complex amplitudes at the receiver outputs. For autocorrelation measurements of the received signal $w_o = v_o$ whereas v_o, w_o corresponds to separate receiver channels for crosscorrelation. The backscattered signal is embedded in receiver and background noise. Assuming the noise contribution to be additive

$$v_o(t) = v_{os}(t) + v_{on}(t) \qquad (2.23)$$

$v_{os}(t)$: backscattered signal

$v_{on}(t)$: noise

and v_{os}, v_{on} to be statistically independent, it follows:

$$R_o(\tau,t) = E\left[v_{os}^*(t-\tfrac{\tau}{2})\ w_{os}(t+\tfrac{\tau}{2})\right] + E\left[v_{on}^*(t-\tfrac{\tau}{2})\ w_{on}(t+\tfrac{\tau}{2})\right] \qquad (2.24)$$

Equation 2.24 is valid provided the ensemble averages of the amplitudes are zero. The stochastic process generating the noise can be regarded time-stationary:

$$E\left[v_{on}^*(t-\tfrac{\tau}{2})\ W_{on}(t+\tfrac{\tau}{2})\right] = R_{on}(\tau) \qquad (2.25)$$

This implies that the noise contribution to R_c can be estimated separately when the backscattered signal is not present, and the estimation with signal and noise can be corrected for the noise contribution. For an observational scheme using separate channels corresponding to orthogonal polarizations, $R_{on}(\tau) = 0$

The backscattered signal from the ionosphere is not time-stationary because of the altitude discrimination which is required for monostatic radar measurements. Assuming, however, the scattering process is time-stationary for scattering volumes corresponding to the time-duration of the transmitted signal, it follows that the received signal at corresponding time-delays in the interpulse period are noise-corrupted and truncated realizations of the scattering process.
Provided the stochastic processes are ergodic, the ensemble average in eq. 2.22 can be replaced by time average for t fixed. Let the variable t denote the relative time-delay in the interpulse period, equation 2.22 can be rewritten:

$$R_o(\tau;t_1) = E\left[v_o^*(t_1-\tfrac{\tau}{2})w_o(t_1+\tfrac{\tau}{2})\right] = E_t\left[v_o^*(t_1-\tfrac{\tau}{2})w_o(t_1+\tfrac{\tau}{2})\right]$$

(2.26)

E_t: time average

The equation states that the correlation function R_o for τ, t_1 fixed can be determined by an estimator based on time-averaging the sample-products $v_o \times w_o$. In order to make optimum use of the available information the time-average should be based on all received amplitudes which contain the realization of the scattering process corresponding to the scattering volume. Denoting the rangegate width τ_g and the estimate of R_o from a single interpulse period $\hat{R}$, the necessary arithmetic operation of the estimator is:

$$\hat{R}(\tau;t_1) = \frac{1}{\tau_g - |\tau|} \int_{-\frac{1}{2}(\tau_g-|\tau|)}^{\frac{1}{2}(\tau_g+|\tau|)} v_o^*(t_1-\alpha-\tfrac{\tau}{2})\, w_o(t_1-\alpha+\tfrac{\tau}{2})\, d\alpha \qquad (2.27)$$

$$|\tau| < \tau_g$$

In order to make full use of the available information in the interpulse period the arithmetic operation should be performed for a large number of rangegates. Denoting the number of interpulse periods N_{ip}, the estimation of the correlation functions is based on:

$$\frac{1}{N_{ip}} \sum_{N_{ip}} \hat{R}(\tau,t_1) \qquad (2.28)$$

N_{ip}: no. of interpulse periods.

In the following only autocorrelation function measurements are considered because the required algorithms for auto- and cross-correlation are in principle the same.

2.3.1. "SINGLE-PULSE" - ALGORITHM

Rangegate considerations:

In the single-pulse mode the rangegate width τ_g is determined by the time-duration τ_T of the transmitted pulse:

$$\tau_g = \tau_T \tag{2.29}$$

The resulting altitude weight-function, in the case when receiver system effects are neglected, will not be uniform as given in fig. 2.1 but will have a triangular shape as sketched in fig. 2.5.

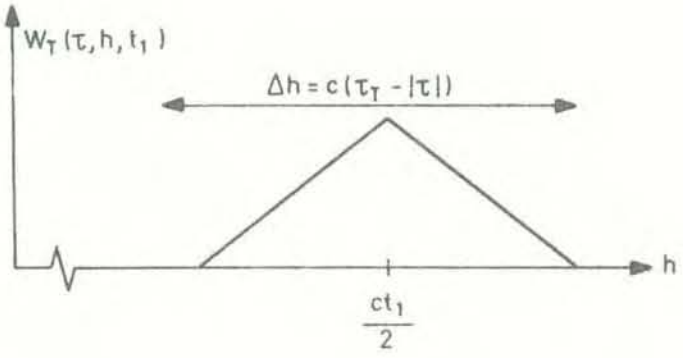

Figure 2.5. Resulting altitude weight-function for the single-pulse mode. Receiver system effects have been neglected.

Because of the non-uniform weighting inside the scattering volume each altitude component will not contribute with the same weight. In figure 2.6 are plotted (solid lines) the resulting altitude weight-functions from rangegates placed side by side for the case $\tau = \tau_T/2$. A gain of information is obtained by having additional rangegates overlapped (dotted lines).

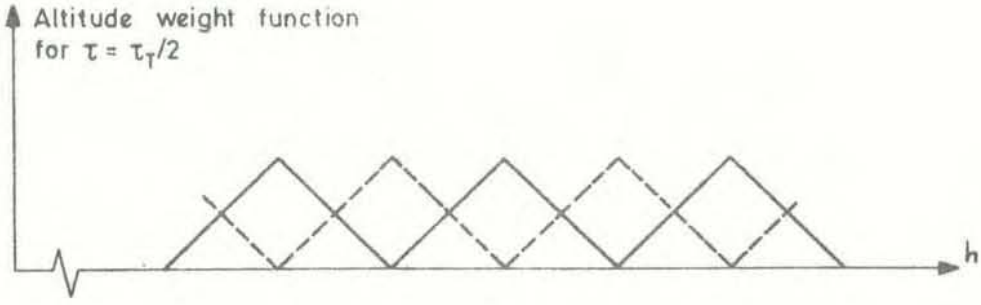

Figure 2.6. Altitude weight-functions for $\tau = \frac{\tau_T}{2}$
Overlapped rangegates.

For the description of the required algorithms discrete time and continuous amplitude representation are used.

Denoting the number of samples (complex) inside a rangegate N_{sg}, the number of rangegates in an interpulse period N_{rg} and the sampling interval Δt, the required algorithm for the singlepulse mode is:

$$\hat{R}_{\ell,r,j} = \sum_{i=0}^{N_{sg}-1-\ell} Z_i \cdot Z^*_{i+\ell} + \hat{R}_{\ell,r,j-1} \qquad (2.30)$$

$$0 \leq \ell \leq N_{sg}-1$$

$i = 0,1,\ldots,N_{sg}-1$: sample index
$\ell = \ell \cdot \Delta t = \tau$: lag parameter
$r = 1.2\ldots\ldots,N_{rg}$: rangegate index
$j = 1,2\ldots\ldots,N_{ip}-1$: index for interpulse period
$Z = v_o(t_1 - \frac{\tau}{2} + i\Delta t)$: complex sample

The normalization constants ahead of the summation have been neglected because the estimate can be normalized by post-processing. An index which has been suppressed in eq. 2.30 is the IF channel number. For experiments using multiple

frequency operation and provided the same waveform is transmitted at the different centre frequencies, the estimate is obtained by:

$$\hat{R}_{\ell,r,j} = \frac{1}{i} \sum_{i} \hat{R}_{\ell,r,j,f_i} \qquad (2.31)$$

$1 \leq i \leq 8$: no. of centre frequencies

The indicated normalization is not strictly correct. As given in eq. 2.2 the correlation function is dependent on the applied radar centre frequency. In order to have a correct lag-parameter scale before the indicated normalization is performed, each scale should be corrected by the multiplication-factor:

$$\frac{f_i}{f_o}$$

f_i: applied frequency

f_o: frequency where the normalization is performed.

In an estimation scheme where the estimates are discrete, this has to be performed by interpolation. The indicated normalization procedure requires that the estimates from the different receiver channels, under certain conditions, have to be kept separate before the normalization in eq. 2.31 is performed.

Sampling considerations:

The sampling frequency $f_s = \frac{1}{\Delta t}$ is determined by the bandwidth of the received complex amplitude (the sampling theorem). Using the expression in eq. 2.17 for the receiver bandwidth, the number of complex samples in a rangegate of width τ_T is given by:

$$N_{sg} = k_f(2+B\cdot\tau_T) \qquad (2.32)$$

B: spectral -width of ionic component.

The constant k_f ($k_f > 1$) is the ratio between the required sampling rate and the theoretical Nyquist rate for reducing foldover-effects of spectra introduced by the sampling process. The constant is given by the pass/stop-band characteristics of the receiver filters.

2.3.2. "MULTIPLE-PULSE" - ALGORITHM

Rangegate and sampling considerations:

The dominant contribution to altitude smearing is sketched in figure 2.4. For the multiple-pulse mode the rangegate corresponds to a set of single samples. This is shown in fig. 2.7 for the four-pulse group given in fig. 2.3. The sampling interval Δt now determines the sampling of the correlation function as a function of altitude. The sampling interval must, however, be given by

$$\Delta t = \frac{\tau_1}{n} \qquad n = 1,2,... \qquad (2.33)$$

in order to obtain the necessary set of samples from the same altitude. Assuming $\Delta t = \tau_e$, the element pulse length, the altitude weighting is approximately the same as the structure given in fig. 2.6 with overlapped rangegates.

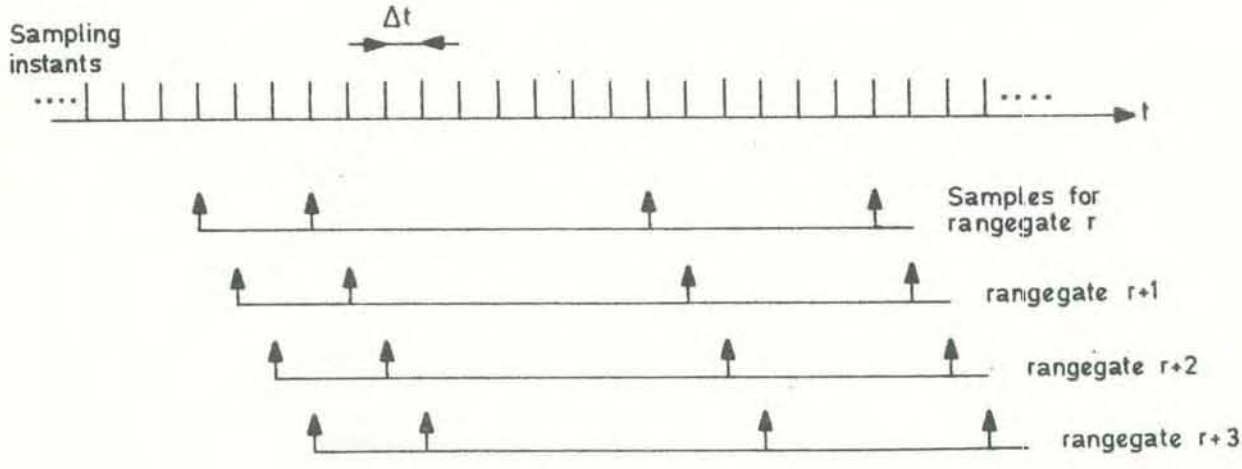

Figure 2.7. Samples defining rangegates in the multiple-pulse mode. Example with a four-pulse group (fig. 2.3.) for

$$\tau_e = \frac{\tau_1}{3}, \quad \Delta t = \tau_e$$

The required algorithm for the multiple-pulse mode is (same notations as in eq. 2.30):

$$\hat{R}_{\ell,r,j} = Z_r \cdot Z^*_{r+\ell} + \hat{R}_{\ell,r,j-1} \qquad (2.34)$$

ℓ equal to all interpulse spacings
Z_r: sample index = range index

In a multiple-pulse experiment using several centre frequencies eq. 2.31 is valid.

2.4. STATISTICAL CONSIDERATIONS.

The quality of the estimate is given by the integration time required to obtain a desirable statistical accuracy. In the following subsections simplified expressions for the variance of the estimates at the receiver output are derived and optimum operations of the radar system are discussed. For simplicity the statistical analysis is based on a model using real signals. At the end of the section generalized expressions for complex signals are given. Both the signal and noise are assumed to be realizations of Gaussian stochastic processes.

2.4.1. SINGLE-PULSE MODE.

The estimate computed for a given interpulse period j, rangegate r and lag ℓ is (for one frequency channel):

$$\hat{R}_{\ell,r,j} = \frac{1}{N_{sg}-\ell} \sum_{i=M}^{M+N_{sg}-1-\ell} Z_i \, Z_{i+\ell} \qquad \begin{matrix} 0 \leq \ell \leq N_{sg}-1 \\ 0 \leq r \leq N_{rg}-1 \end{matrix}$$

where

N_{rg}: No. of rangegates in interpulse period

N_{sg}: No. of samples in rangegate

i : Sample index in interpulse period

$$M = \begin{cases} r \cdot N_{sg} & \text{no overlapped rangegates} \\ \frac{r}{2} \cdot N_{sg} & \text{overlapped rangegates, } N_{sg} \text{ even} \\ \frac{r}{2} \cdot N_{sg} & \text{overlapped rangegates, } N_{sg} \text{ odd, r even} \\ \frac{r}{2} \cdot N_{sg} - \frac{1}{2} & \text{overlapped rangegates, } N_{sg} \text{ odd, r odd} \end{cases}$$

For the last rangegates in the interpulse period sampling only on background and receiver-system noise is assumed. The noise estimation is not altitude-dependent so the noise estimates for same ℓ can be added over several gates. The noise estimates from interpulse period j can be expressed as:

$$\hat{R}_{\ell,n,j} = \frac{1}{N_1 - \ell} \sum_{i=M_1}^{M_1+N_1-1-\ell} Z_i \cdot Z_{i+\ell}$$

where $N_1 = k \cdot N_{sg}$, $k \geq 1$ and $M_1 >> 1$.

Over a total of N_{ip} interpulse periods the scan-to-scan integration gives:

$$\text{RANGEGATE ESTIMATE} \quad \hat{K}_1 = \frac{1}{N_{ip}} \sum_{j=1}^{N_{ip}} \hat{R}_{\ell,r,j}$$

$$\text{NOISE ESTIMATE} \quad \hat{K}_2 = \frac{1}{N_{ip}} \sum_{j=1}^{N_{ip}} \hat{R}_{\ell,n,j} \qquad (2.35)$$

The noise-corrected estimate of the autocorrelation function corresponding to the backscattered signal is:

$$\hat{K} = \hat{K}_1 - \hat{K}_2 \qquad \text{(for all } \ell\text{)} \qquad (2.36)$$

The estimate $\hat{K}$ is a biased estimate of the plasma autocorrelation function (eq. 2.11). The estimates $\hat{K}_1$ and $\hat{K}_2$ are statistically independent and the variance of $\hat{K}$ is given by:

$$\mathrm{VAR}(\hat{K}) \triangleq E\left[(\hat{K}-E[\hat{K}])^2\right] = \mathrm{VAR}(\hat{K}_1) + \mathrm{VAR}(\hat{K}_2) \tag{2.37}$$

$\hat{R}_{\ell,r,j}$ is independent of $\hat{R}_{\ell,r,k}$ if $k \neq j$, and the same holds for $\hat{R}_{\ell,n,j}$, and for a given rangegate:

$$\mathrm{VAR}(\hat{K}_1) = \frac{1}{N_{ip}}\mathrm{VAR}(\hat{R}_\ell) = \frac{1}{N_{ip}}\left(E[\hat{R}_\ell^2] - E[\hat{R}_\ell]^2\right) \qquad (\hat{R}_\ell = \hat{R}_{\ell,r,j}) \tag{2.38}$$

$$\mathrm{VAR}(\hat{K}_2) = \frac{1}{N_{ip}}\mathrm{VAR}(\hat{R}_{\ell,n})$$

The second-order moment of R_ℓ is given by:

$$E[\hat{R}_\ell^2] = \frac{1}{(N_{sg}-\ell)^2}\sum_{i=0}^{N_{sg}-1-\ell}\sum_{k=0}^{N_{sg}-1-\ell} E[Z_i Z_{i+\ell} Z_k Z_{k+\ell}] \tag{2.39}$$

The fourth-order moment of a Gaussian distribution is (provided $E[Z] = 0$):

$$E[Z_i Z_{i+\ell} Z_k Z_{k+\ell}] = E[Z_i Z_{i+\ell}]E[Z_k Z_{k+\ell}] + E[Z_i Z_k]E[Z_{i+\ell} Z_{k+\ell}] + E[Z_i Z_{k+\ell}]E[Z_{i+\ell} Z_k] \tag{2.40}$$

Using the notation $E[Z_i Z_{i+\ell}] = R_\ell$:

$$E[\hat{R}_\ell^2] = \frac{1}{N_{sg}-\ell}\left(R_o^2 + 2R_\ell^2\right) + \frac{1}{(N_{sg}-\ell)^2}\sum_{\substack{i \\ k\neq i}}\sum_{k} E[Z_i Z_{i+\ell} Z_k Z_{k+\ell}] \tag{2.41}$$

The last term in 2.41 can be simplified by using $R_{-\ell} = R_{\ell}$:

$$\frac{1}{(N_{sg}-\ell)^2} \sum_{i} \sum_{\substack{k \\ k\neq i}} (R_{\ell}^2 + R_{k-i}^2 + R_{k+\ell-i}R_{k-\ell-i})$$

$$= \frac{N_{sg}-1-\ell}{N_{sg}-\ell} R_{\ell}^2 + \frac{2}{(N_{sg}-\ell)^2} \sum_{i=1}^{N_{sg}-1-\ell} (N_{sg}-\ell-i)[R_i^2 + R_{i+\ell}R_{i-\ell}] \tag{2.42}$$

The mean value of $\hat{R}_{\ell}$ is given by:

$$E[\hat{R}_{\ell}] = R_{\ell} \tag{2.43}$$

Finally:

$$VAR(\hat{K}_1) = \frac{1}{N_{ip}(N_{sg}-\ell)} (R_o^2 + R_{\ell}^2) + \frac{2}{N_{ip}(N_{sg}-\ell)^2} \sum_{i=1}^{N_{sg}-1-\ell}$$

$$(N_{sg}-\ell-i)[R_i^2 + R_{i+\ell}R_{i-\ell}] \tag{2.44}$$

Equation 2.44 shows that the estimate is consistent considering the extraction of noise-corrupted autocorrelation function at the receiver output. The last term in 2.44 is caused by the correlation between samples and is determined by the actual autocorrelation function to be estimated and the sampling rate. The minimum value of the variance is reached when the samples are uncorrelated, for the power estimate:

$$VAR_{\ell=0} (\hat{K}_1)_{MIN} = \frac{2R_o^2}{N_{ip} \cdot N_{sg}} \tag{2.45}$$

For all other lags:

$$VAR_{\ell\neq 0} (\hat{K}_1)_{MIN} = \frac{R_o^2}{N_{ip}(N_{sg}-\ell)} \tag{2.46}$$

As the value of the lag parameter approaches N_{sg}, the variance of the estimate increases. This results from the fact that the estimate is based on computing the sample mean of the sequence $Z_o,\ldots,Z_{N_{sg}-1}$. If ℓ is of the order of N_{sg}, then there are only a few products available pr. rangegate.

The signal samples are embedded in statistically independent noise:

$$R_\ell = R_{\ell,s} + R_{\ell,n} \tag{2.47}$$

By the notations:

$$\begin{aligned} R_{\ell,s} &= P_s \cdot \rho_{\ell,s} \\ R_{\ell,n} &= P_n \cdot \rho_{\ell,n} \\ SNR &= \frac{P_s}{P_n} \end{aligned} \tag{2.48}$$

the variance normalized to the square of the received signal power is:

$$\frac{VAR(\hat{K}_1)}{P_s^2} = \frac{(1+SNR^{-1})^2}{N_{ip}(N_{sg}-\ell)} \left\{1+\rho_\ell'^2 + 2\sum_{i=1}^{N_{sg}-1-\ell}(1-\frac{i}{N_{sg}-\ell})\left[\rho_i'^2+\rho_i''\right]\right\}$$

$$\rho_\ell' \triangleq \frac{P_s\rho_{\ell,s} + P_n\rho_{\ell,n}}{P_s + P_n} \tag{2.49}$$

$$\rho_i'' \triangleq \frac{(P_s\rho_{i-\ell,s} + P_n\rho_{i-\ell,n})\ (P_s\rho_{i+\ell,s} + P_n\rho_{i+\ell,n})}{(P_s + P_n)^2}$$

Defining the effective number of lagged products in the rangegate:

$$N_g \triangleq \frac{N_{sg}-\ell}{N} \tag{2.50}$$

where N is defined by the bracket $\{\cdot\}$ in 2.49, it follows:

$$\frac{VAR(\hat{K}_1)}{P_s^2} = \frac{(1+SNR^{-1})^2}{N_{ip} \cdot N_g} \qquad (2.51)$$

The variance of the noise-corrected estimate can be determined using a similar form of $VAR(K_2)$ as in 2.51.

Practical considerations:

Provided SNR << 1, the sampling rate is given to meet the Nyquist requirement, and for $\ell \neq 0$:

$$N_g \approx N_{sg} - \ell \quad (N_{sg} \text{ given by eq. 2.17}) \qquad (2.52)$$

the variance of the estimate $\hat{K}$ is given by:

$$\frac{VAR(\hat{K})}{P_s^2} \quad \frac{SNR^{-2}}{N_{ip}(N_{sg}-\ell)} \left(1 + \frac{N_{sg}-\ell}{N_1-\ell}\right) \qquad (2.53)$$

$N_1 - \ell$ is the number of lagged products on the noise, and an effective scheme is to let $N_1 >> N_{sg}$, i.e. performing as many lagged products on the noise samples as other considerations permit.

The SNR dependence on the factor N in 2.50 is not strong for $\ell > 1$. For a desired accuracy of K it follows that the required number of interpulse periods is propotional to $(1+SNR^{-1})^2$:

$$N_{ip} \propto (1+SNR^{-1})^2 \qquad (2.54)$$

The signal-to-noise ratio SNR is proportional to the transmitted peak power P_T. Using a single frequency scheme it is optimal to make $P_T = P_{T,MAX}$ but the relative decrease in N_{ip} is marginal provided SNR > 1. In this case the available transmitter power should be distributed to other centre frequencies in a multiple-frequency scheme. Adopting this method the number of interpulse periods will be reduced by a factor equal to the number of frequencies transmitted provided the different receiver channel estimates are statistically independent. The optimum scheme to be followed can be explained by this example:

The observation is defined by the observational altitude range

and the desirable altitude-resolution, which in the single-pulse mode defines the time-duration of the transmitted pulse. The required interpulse period T is given by the observational range and time-interval for the noise estimation. Assuming that the peak power is $P_T = P_{T\ MAX}$ and the signal-to-noise ratio is SNR, then for a desirable accurate estimate the required number of interpulse periods is fixed. The actual average power transmitted is

$$\frac{P_{TMAX} \cdot \tau_T}{T} = P_M \qquad (2.55)$$

By reducing the peak power by a factor X, it follows that for the same average power the pulse can be repeated at X centre frequencies in sequence, provided the time-duration of the total transmitted signal does not diminish the observation interval. The required number of interpulse periods for the same total accuracy is given by:

$$N_{ip} \alpha (1+X \cdot SNR^{-1})^2 \cdot X^{-1} \qquad (2.56)$$

The optimum observational scheme is given by:

$$N_{ip,MIN} \Rightarrow X = SNR \qquad (2.57)$$

This implies that whenever SNR > 1 the optimum scheme is to operate the radar in a multiple-frequency mode by reducing the SNR in each receiver channel to 1. The optimum operational mode also makes use of the maximum available average power by operating the radar at the full duty-cycle. This can be fulfilled by adding extra frequencies. If other considerations prohibit this, the given frequencies should be transmitted with the maximum available peak-power.

The required number of interpulse periods for electron density observations (zero-lag estimation) are related to the SNR as given in eq. 2.54. If the transmitted pulse length $\tau_T < \tau_M$; the plasma correlation time, it follows that the noise power is inverse-propotional to τ_T, while the received

signal power is propotional to τ_T. The pulse length determines the range-resolution:

$$N_{ip} \alpha (\Delta h)^{-4} \qquad (2.58)$$

Δh: range-resolution
SNR << 1

Instead of decreasing the pulse energy, range-resolution can be obtained by phase-coding. In this case

$$N_{ip} \alpha (\Delta h)^{-2} \qquad (2.59)$$

phase-coding
SNR << 1

2.4.2. MULTIPLE-PULSE MODE

For this mode only single sample-products are generated. For a given interpulse period j, rangegate r (= sample index) and lag ℓ, the rangegate estimate is:

$$\hat{R}_{\ell,r,j} = Z_r \cdot Z_{r+\ell}$$

The noise estimation can, in principle, be computed from several sample-products for a given lag:

$$\hat{R}_{\ell,n,j} = \frac{1}{N_1} \sum_{i=M_1}^{M_1+N_1} Z_i Z_{i+\ell}$$

where $N_1 \geq 1$ and $M_1 >> 1$.

Calculation of the variance corresponding to the estimate $\hat{K}_1$ in eq. 2.35 gives:

$$VAR(\hat{K}_1)_{\ell \neq 0} \approx \frac{1}{N_{ip}} \left\{ (R_{o,s} + R_{o,n})^2 + R_{\ell,s} \right\} \qquad (2.60)$$

The receiver bandwidth is determined by the element pulse of the pulse group, thus the autocorrelation function $R_{\ell,n}$ is negligible for $\ell >> 1$. For the signal autocorrelation function:

$$R_{\ell,s} \alpha P_T \quad \text{for } \ell \neq o \quad \text{(equal to interpulse spacings)}$$

$$R_{o,s} \alpha n_p \cdot P_T, \quad n_p\text{: no. of element pulses} \tag{2.61}$$

With the normalizations:

$$\begin{aligned} R_{\ell,s} &= P_s \rho_{\ell,s} \qquad \ell \neq 0 \\ R_{o,s} &= n_p P_s \qquad \ell = 0 \\ P_{\ell,n} &= P_n \rho_{\ell,n} \end{aligned} \tag{2.62}$$

$$SNR = \frac{P_s}{P_n}$$

the normalized variance is given by:

$$\frac{VAR(\hat{K}_1)}{P_s^2} \approx \frac{1}{N_{ip}} \left\{ (n_p + SNR^{-1})^2 + \rho_{\ell,s}^2 \right\} \tag{2.63}$$

For a desired statistical accuracy and $\ell >> 1$ the number of interpulse periods is given by:

$$N_{ip} \alpha (n_p + SNR^{-1})^2 \tag{2.64}$$

Transmitting the pulse-group at X frequencies:

$$N_{ip} \alpha (n_p + X\, SNR^{-1})^2 X^{-1} \tag{2.65}$$

X: no. of frequencies

$$N_{ip,MIN} \Rightarrow X = SNR \cdot n_p \tag{2.66}$$

The optimum requirement can be rewritten:

$$X = \frac{P_s + (n_p - 1)P_s}{P_n} \qquad (2.67)$$

P_s is the power of the signal to be detected. The term $(n_p-1)\cdot P_s$ is introduced by the other pulses in the group and may be regarded as a "self"-clutter signal with power proportional to the transmitted peak power. Eq. 2.67 states that whenever $P_s + P_{s,clutter}$ exceeds the power of the noise, it is more efficient to distribute the available power to pulse-groups at other transmitted frequencies.

2.4.3. COMPLEX SIGNAL REPRESENTATION

In the EISCAT system the complex amplitude of the bandlimited signal is detected by a syncronous demodulation scheme using a quadrature hybrid, ref. [10]. A block-diagram of the idealized baseband demodulation is given in figure 2.8. The signal at IF can be expressed as:

$$f_{IF}(t) = \mathrm{Re}\left\{ v_o(t) e^{\,j2\pi f_o t} \right\} \qquad (2.68)$$

$$= x(t)\cos 2\pi f_o t - y(t)\sin 2\pi f_o t$$

f_o: IF centre frequency

$x(t) = \mathrm{Re}\{v(t)\}$: in-phase component

$y(t) = \mathrm{Im}\{v(t)\}$: quadrature component

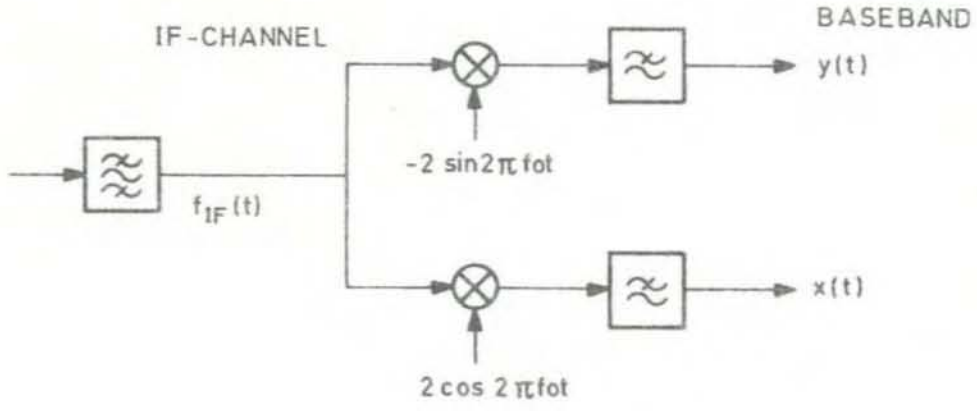

Figure 2.8. Demodulation scheme for one frequency channel in the radar receiver.

The complex autocorrelation function of the amplitude is:

$$R_o(t) \triangleq E\left[v_o^*(t-\tfrac{\tau}{2}) v_o(t+\tfrac{\tau}{2}) \right]$$

$$= E\left[x(t-\tfrac{\tau}{2})x(t+\tfrac{\tau}{2}) + y(t-\tfrac{\tau}{2})y(t+\tfrac{\tau}{2}) \right] \qquad (2.69)$$

$$+jE\left[x(t-\tfrac{\tau}{2})y(t+\tfrac{\tau}{2}) - y(t-\tfrac{\tau}{2})x(t+\tfrac{\tau}{2}) \right]$$

Using a discrete time notation

$$\mathrm{Re}\{R_\ell\} = E\left[x_i x_{i+\ell} + y_i y_{i+\ell} \right]$$

$$\mathrm{Im}\{R_\ell\} = E\left[x_{i+\ell} y_i - x_i y_{i+\ell} \right] \qquad (2.70)$$

By detection of the quadrature components of the complex amplitude, the estimator for extracting the real and imaginary part of R_ℓ is based on time-averaging the sample products given in eq. 2.70.

For the single-pulse mode the rangegate estimators have the algorithms (indexes of samples for rangegate r):

REAL PART ESTIMATE

$$\hat{R}_{\ell,r,j,re} = \frac{1}{N_{sg}-\ell} \sum_{i=0}^{N_{sg}-1-\ell} (X_i X_{i+\ell} + Y_i Y_{i+\ell})$$

IMAGINARY PART ESTIMATE (2.71)

$$\hat{R}_{\ell,r,j,im} = \frac{1}{N_{sg}-\ell} \sum_{i=0}^{N_{sg}-1-\ell} (X_{i+\ell} Y_i - X_i Y_{i+\ell})$$

N_{sg}: no. of complex samples in rangegate

ℓ: lag index

r: rangegate index

j: interpulse period index.

Calculations of the variance give the result:

$$VAR(\hat{R}_{\ell,r,j,re}) = \frac{1}{2(N_{sg}-\ell)} \left[(ReR_o)^2 + (ReR_\ell)^2 - (ImR_\ell)^2 \right]$$

$$+ \frac{1}{(N_{sg}-\ell)^2} \sum_{i=1}^{N_{sg}-1-\ell} (N_{sg}-\ell-i) \left[(ReR_i)^2 + (ImR_i)^2 + ReR_{i-\ell} \cdot ReR_{i+\ell} + ImR_{i-\ell} \cdot ImR_{i+\ell} \right] \quad (2.72)$$

$$VAR(\hat{K}_{\ell,r,j,im}) = \frac{1}{2(N_{sg}-\ell)} \left[(ReR_o)^2 + (ImR_\ell)^2 - (ReR_\ell)^2 \right]$$

$$+ \frac{1}{(N_{sg}-\ell)^2} \sum_{i=1}^{N_{sg}-1-\ell} (N_{sg}-\ell-i) \left[(ReR_i)^2 + (ImR_i)^2 - ReR_{i-\ell} \cdot ReR_{i+\ell} - ImR_{i-\ell} \cdot ImR_{i+\ell} \right] \quad (2.73)$$

After N_{ip} interpulse periods the normalized variance for $\ell >> 1$ is (see eq. 2.35):

$$\frac{VAR(\hat{K}_{1,re})}{(ReR_o)^2} \approx \frac{1}{2N_{ip}(N_{sg}-\ell)} (1+SNR^{-1})^2 \quad , \ \ell >> 1 \qquad (2.74)$$

The number of "effective" complex samples in the rangegate is given in eq. 2.32 with $k_f = 1$. ($\tau_T >> \tau_M$ has been assumed). For the imaginary part the normalized variance $VAR(\hat{K}_{1,im}) / (ReR_o)^2$ has the same form as given in eq. 2.74.

The same computations as above can be performed for the multiple-pulse mode assuming only one sample-product is performed in the rangegate for a given ℓ. The variance is approximately:

$$\frac{VAR(\hat{K}_{1,re})}{(ReR_o)^2} \approx \frac{1}{2N_{ip}} (n_p+SNR^{-1})^2 \qquad (2.75)$$

n_p: no. of element pulses.

2.5. CALCULATIONS FOR SPECIFIC EXAMPLES

In this section two examples for operation of the UHF-system are considered (monostatic observations):

(α) Single-pulse experiment for estimation of the autocorrelation function of the ionic component in the altitude region: 700-1000 km.
Desirable range-resolution: 75 km.

(β) Multiple-pulse experiment (5 pulse group) for observations at 120 km, range-resolution: 2 km.

The required integration time is computed in this case: determination of the autocorrelation function corresponding to the backscattered signal and noise at the receiver output with an assumed true value of 0.5 compared with the zero-lag value and a r.m.s. accuracy (normalizied to the true value) of 1%. Systematic errors due the analogue receiver system and data-acquisition elements have been neglected.

2.5.1. THE RADAR-EQUATION FOR MONOSTATIC OBSERVATIONS

The power density at the scattering volume at a distance R from the antenna is:

$$\frac{P_T \cdot G_T}{4\pi R^2} \tag{2.76}$$

P_T: peak power

G_T: antenna gain

The backscattered power density at the antenna is:

$$\frac{P_T \cdot G_T}{4\pi R^2} \cdot \frac{N_o V \sigma_e}{4\pi R^2} \tag{2.77}$$

N_o: electron density

V : scattering volume

σ_e: effective cross-section of an electron

The scattering volume can be expressed by:

$$V = \frac{4\pi R^2}{G_T} \cdot \Delta h = \frac{4\pi R^2}{G_T} \cdot \frac{c \cdot \tau_T}{2} \tag{2.78}$$

τ_T: pulse length

The instantanously received power is:

$$P_s = \frac{L \cdot P_T \cdot A \cdot c}{8\pi R^2} \cdot N_o \sigma_e \cdot \tau_T \tag{2.79}$$

A: antenna aperture

L: receiver loss

The noise power is:

$$P_n = kTB_R \tag{2.80}$$

k: Boltzmann's constant

T: noise temparature

B_R: eq. noise bandwidth

The signal-to-noise ratio SNR is then:

$$SNR \triangleq \frac{P_S}{P_n} = \frac{L \cdot P_T \cdot A \cdot c}{8\pi kT} \cdot \sigma_e N_o \cdot \frac{\tau_T}{B_R \cdot R^2} \tag{2.81}$$

An approximate expression for σ_e can be found in ref. [2] (valid for $\alpha << 1$):

$$\sigma_e = \frac{4\pi r_o^2 \sin^2 x}{(1+\alpha^2)(1+T_e/T_i+\alpha^2)} \tag{2.82}$$

r_o: classical electron radius ($2.84 \cdot 10^{-15}$ m)

x : polarization angle

T_e/T_i : electron/ion-temp. ratio.

$\alpha = \frac{4\pi h_p}{\lambda_T}$, h_p: Debye-length

λ_T: radar wave-length

For the ionospheric models in ref.[5] and circular polarization:

Altitude 1000 km:

Mean model: $N_o = 7 \cdot 10^{10}\ m^{-3}$, $\sigma_e = 2.933 \cdot 10^{-29}\ m^2$

Altitude 120 km:

Mean model: $N_o = 1.5 \cdot 10^{11} m^{-3}$, $\sigma_e = 4.958 \cdot 10^{-29}\ m^2$

Minimum model: $N_o = 2 \cdot 10^{10}\ m^{-3}$, $\sigma_e = 4.325 \cdot 10^{-29}\ m^2$

The UHF-system parameters:

$$P_T = 2MW$$

$$A = 518.6\ m^2 \quad (48dB\ gain)$$

$$T = 50^0\ K$$

$$L = 0.8$$

$$SNR_{UHF} = 1.435 \cdot 10^{37} \cdot \sigma_e N_o \cdot \frac{\tau_T}{B_R \cdot R^2} \qquad (2.83)$$

2.5.2. SINGLE-PULSE EXPERIMENT(α)

The desirable range-resolution 75 km determines the transmitted pulse-length:

$$\tau_T = 0.5\ msec$$

The receiver bandwidth is given in table II.2 : $B_R = 38$ kHz

With maximum peak-power transmitted the SNR is:

Mean model: SNR = 0.39

Provided a sampling frequency $f_s = 50$ kHz (simultaneously sampling on the quadrature components), 25 point-estimates (complex) can be obtained in a rangegate. The observational altitude-region is given by

700 - 1000 km → 4.67 - 6.67 msec.

Assuming the pulse repetition time is limited by the required background noise estimation to:

$T_{min} = 16.67$ msec → 2500 km.

The duty cycle for single-pulse transmissions is:

$$\frac{\tau_T}{T_{min}} = 0.03 \qquad (24\ \%\ of\ full\ cycle).$$

which implies that 4 frequencies can be applied with τ_T = 0.5 msec and maximum peak-power. The number of independent samples is approximately:

$$N = \left(\frac{2}{\tau_T} + B\right) \cdot \tau_T = 19$$

Assuming that for $\ell = 1$: $R_\ell/R_o = 0.5$, it follows for a statistical accuracy of 1%:

$$\text{number of interpulse periods } N_{ip} \approx \frac{(1+0.39^{-1})^2}{0.01^2 \cdot 0.5^2 \cdot 4 \cdot 18 \cdot 2} = \underline{3529}$$

The total integration time becomes (mean model): 58.8 sec.

2.5.3. MULTIPLE-PULSE EXPERIMENT (β)

The required altitude-resolution 2 km determines the element pulse length

$$\tau_T \approx 13 \text{ μsec.}$$

The receiver bandwidth is $1/\tau_T$ = 75 kHz. With maximum peak power transmitted the SNR is:

Mean model: 1.28 Minimum model: 0.15

For a five pulse group the number of complex point-estimates pr. rangegate is 10. Provided a minimum spacing of element pulses τ_1 = 52 μsec (see fig. 2.3), the autocorrelation function can be estimated for lags:

$$\ell \cdot 52 \text{ μsec}, \quad \ell = 1,2,.....,10$$

With the example given it is possible to transmit the pulse-group at 4 frequencies by frequency-commutate the element pulse (13 μsec). Compared with the delay-time for 120 km: 0.8 msec, the total length of the transmitted signal is 0.572 msec. This implies that a new group at 4 other frequencies can be transmitted after the first one. In this case the limiting factor

for the transmitter is the maximum repetition rate 1 kHz. Provided that 4 element pulses transmitted by frequency-commutation are equvivalent to one pulse, the minimum repetition time is 5 msec. (750 km). The signal-to-noise ratio from signals at the same frequencies (1620 km) is $7 \cdot 10^{-3}$. The duty cycle is

$$\frac{4 \cdot 5 \cdot 13 \cdot 10^{-6}}{5 \cdot 10^{-3}} = 0.052 \quad (41.6\% \text{ of full cycle})$$

For the mean model:

$$N_{ip} \quad \frac{(5+1.28^{-1})^2}{0.01^2 \cdot 0.5^2 \cdot 4 \cdot 2} = \underline{167115} \text{ periods} \rightarrow \underline{13.9} \text{ min}$$

For the minimum model, provided 3% statistical accuracy:

$$N_{ip} \quad \frac{(5+0.15^{-1})^2}{0.03^2 \cdot 0.5^2 \cdot 4 \cdot 2} = \underline{75618} \text{ periods} \rightarrow \underline{6.3} \text{ min}$$

CHAPTER 3

DIGITAL CORRELATORS. A COMPARISON OF DIFFERENT TYPES.

In applications where the signal-to-noise ratio at the correlator input is small, the estimation scheme for producing a sufficiently accurate estimate is based on a long integration-time for time-average of a large number of sample-products. A major design-philosophy for the EISCAT system is the optimalization of the observational time-resolution, i.e. minimalization of the integration-time in order to detect time variations in the ionosphere. A second factor which characterizes the monostatic radar observations is the time-gating technique of the received signal for the required range-resolution: The signals in the different rangegates have to be processed separately. A third factor is, for the monostatic measurements, the dynamic variations of the received signal when SNR > 1, and a correlator-concept has to be selected which does not set severe limitations due to dynamic variations. For the EISCAT system an analogue realization of the estimator is not realistic, caused by the inherent stability- and systematic-effects generated by this technique, and the requirements for storing preprocessed data. An analogue solution also sets limitations on the programmability of the device. A digital realization of the correlator fulfils to a large degree the requirements, but also sets basic limitations. Compared with an analogue realization these are the hardware complexity and the data processing speed. Another technique which seems to be attractive is realizing the estimator-processing by software, i.e. perform the necessary arithmetic operations by a programmed special-purpose micro-processor or a high-speed pherical device in a computer system. These systems operate basicly in a serial operational scheme (single operation pr. cycle) which limits the processing speed for on-line applications. The developement-trend for on-line, high-speed processing by software is, however, directed towards multi CPU - (central processing unit) structures realizing "pipe-line" operations (operations performed in sequence) for increased processing speed. With the present status of this technique, the required digital hardware and the strict speed requirements for the EISCAT correlator, only a

digital hardware concept has been considered where the realization is based on operations performed in parallel.

Figure 3.1 gives a sketch of a generalized digital autocorrelator performing the estimation algorithm:

$$\hat{R}_\ell = \frac{1}{N_{sg}-\ell} \sum_{i=0}^{N_{sg}-1-\ell} g_1(Z_i) g_2(Z_{i+\ell}) \qquad (3.1)$$

$$0 \leq \ell \leq N_{sg}-1$$

ℓ : lag parameter

N_{sg} : number of samples in the rangegate.

The sample-values $Z_0, Z_1, \ldots, Z_k$ are digitized and loaded into a digital shiftregister-chain. The digital representation of the present sample is denoted by $g_2(Z_k)$ and the delayed samples $g_1(Z_{k-\ell})$, whereas in the general case $g_1 \neq g_2$. The normalization factor $1/N_{sg}-\ell$ is not included in the digital operations because the scaling operation of the estimates can be performed by computer post-processing. In order to simplify the digital arithmetic modules all computations are performed in integer format.

Parameters which affect the system complexity and speed limitations are:

- the number of binary digits for the present sample and the delayed samples determine the correlator performance, and in section 3.5 comparisons of the required integration time for different types of quantization schemes are made. The number of chosen bits determines the hardware complexity of the shiftregister - and multiplier-chain,
- the number of binary digits for the accumulators and the result-memory locations determines the correlator integration time for preprocessing, a factor which determines the repetition time for dumping preprocessed data to the computer system.

In the following subsections different types of digital correlators are briefly described.

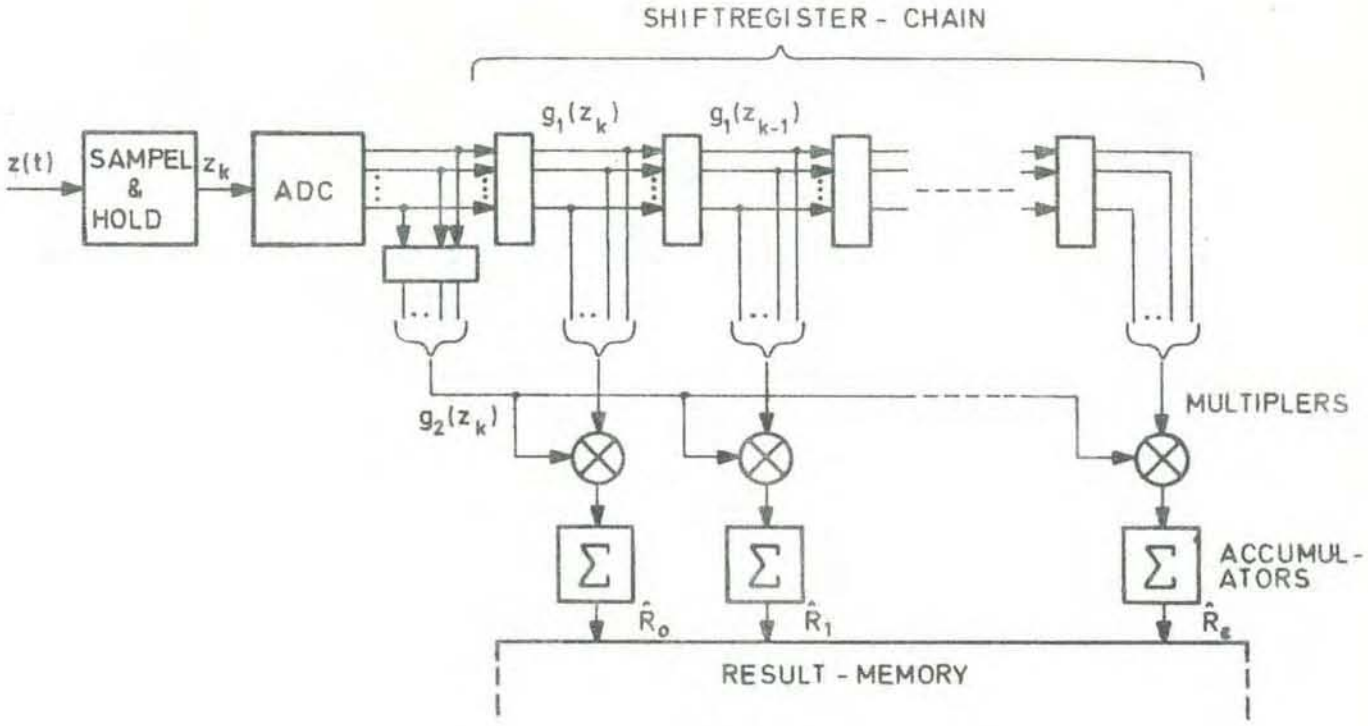

Figure 3.1. Blockdiagram of a generalized digital autocorrelator.

3.1. MULTIBIT CORRELATORS

As given in chapter 2 the normalized statistical error in the estimation of the autocorrelation function is proportional to $1/\sqrt{N}$ where N is the number of sample-products. Due to the discrete representation of the sample-amplitude in a digital system, quantization-noise is introduced. This noise can in general be divided into 3 classes (ref.[11]):

- when the input signal level (power) is small compared with the quantization interval the quantization-effect may be regarded as hard-clipping the signal,
- when the signal level is large compared with the maximum quantization-level, the quantization acts as a linear limiter,

- for signal levels in the linear zone the noise is given by the quantization interval, i.e. the number of bits in the digital representation of the signal.

Operating in the linear zone and assuming a linear quantizaion scheme, reference [11] and [12] show that the estimated autocorrelation function is biased due to the quantization noise. Ref.[12] gives the bias error (approximation):

$$\varepsilon(\tau) = \frac{1}{12}\frac{q^2}{\sigma^2} e^{-\frac{4\pi^2\sigma^2}{q^2}(1-\rho(\tau))} \qquad (3.2)$$

which holds for Gaussian input with variance σ^2 and normalized autocorrelation function $\rho(\tau)$, q is the quantization interval. Clipping effects of the signal are not considered. Assuming the quantization region is limited to $\pm A$, the quantization interval can be written as:

$$q = \frac{2A}{2^m} = A \cdot 2^{-m+1}$$

m: no. of bits for the digital representation of the signal.

For power estimation the bias term is:

$$\varepsilon(0) = \frac{1}{3} 2^{-2m} \left(\frac{A}{\sigma}\right)^2 \qquad (3.4)$$

In table III.1 the error term is computed for m = 6,....,9 for the case $A/\sigma = 3$.

m	6	7	8	9
$\frac{A}{\sigma} = 3$	$7.32 \cdot 10^{-4}$	$1.83 \cdot 10^{-4}$	$4.58 \cdot 10^{-5}$	$1.14 \cdot 10^{-5}$

Table III.1. Biased error due to quantization for a multibit autocorrelator.

The table gives that for $A/\sigma = 3$ the quantization error is negligible compared with the desired statistical accuracy of the estimate ($\sim 1\%$). Assuming that the SNR > 1 at the receiver input and for the altitude range the σ decreases with a factor of 10, then for $A/\sigma = 30$ the values in the table have to be multiplied by 10^2. This illustrates the importance of having as many bits as other considerations permit in case the dynamic range of the input signal is large.

In a multibit correlator the shiftregister-chain is word-organized and the hardware multipliers must perform a signed m x m bit product, the result being 2 m bits.

3.2. ONE-BIT (POLARITY COINCIDENCE) CORRELATORS

With this type of correlator the computations are based only on the sign of the sampled amplitudes, the quantization functions being:

$$g_1(x) = g_2(x) = \operatorname{sgn}(x) \tag{3.5}$$

$$\operatorname{sgn}(x) = \begin{cases} +1 & \text{for } x>0 \\ 0 & \text{for } x=0 \\ -1 & \text{for } x<0 \end{cases}$$

Assuming a Gaussian input and applying Price's theorem, ref. [13], the autocorrelation function estimated is

$$E[\hat{R}(\tau)] = \frac{2}{\pi} \arcsin \rho(\tau) \tag{3.6}$$

$\rho(\tau)$: normalized input autocorrelation function.

Eq. 3.6 shows that the power information of the input signal is lost. In reference [14] the normalized statistical error is computed for $\rho(\tau) \ll 1$:

$$\varepsilon_{\hat{R}} = \frac{\pi}{2} \cdot \frac{1}{\sqrt{N}} = \frac{1.57}{\sqrt{N}} \tag{3.7}$$

The effect of hard-limiting the input signal causes the spectrum to broaden, (ref.[15]) which implies that a gain of information is obtained by oversampling. Assuming the sampling rate is set to two times the Nyquist rate, the error is reduced to [14]:

$$\varepsilon_{\hat{R}} = \frac{1.35}{\sqrt{N}} \qquad \text{OVERSAMPLING} \tag{3.8}$$

The major advantage with the one-bit correlator is the simplified hardware construction. A shiftregister-chain of one bit is required, and the multipliers are not necessary. The accumulators can be realized by up/down binary counters. With this type of correlation high-speed correlators can be realized, the speed limitation is only determined by the maximum clock-rate of the counters.

3.3. HYBRID CORRELATORS

With this scheme only the sign bit is transferred to the shift-register.

$$g_1(x) = \operatorname{sgn}(x)$$

$$g_2(x): \text{ multibit sample}$$

The autocorrelation function estimated is (Gaussian input is assumed) (ref. [14]):

$$E[\hat{R}(\tau)] = \sqrt{\frac{2}{\pi}}\,\sigma\rho(\tau) \tag{3.9}$$

which means that power information is maintained. Quantization effects on the multibit sample are neglected. The statistical error is for $\rho(\tau) \ll 1$:

$$\varepsilon_{\hat{R}} = \frac{1.25}{\sqrt{N}}$$

$$\varepsilon_{\hat{R}} = \frac{1.15}{\sqrt{N}} \qquad \text{OVERSAMPLING} \tag{3.10}$$

For the hybrid scheme no multipliers are necessary and the accumulators must have an add/subtract-control determined by the delayed sign-bit. The speed limitation for this type of correlator is given by the necessary add-time for the accumulators.

3.4. N x M-BIT CORRELATORS

In reference [16] several nxm-bit correlators are considered with the number of bits m,n relatively small.

MULTIBIT BY TWO-BIT:

Assuming a quantizer transfer-function for the delayed samples:

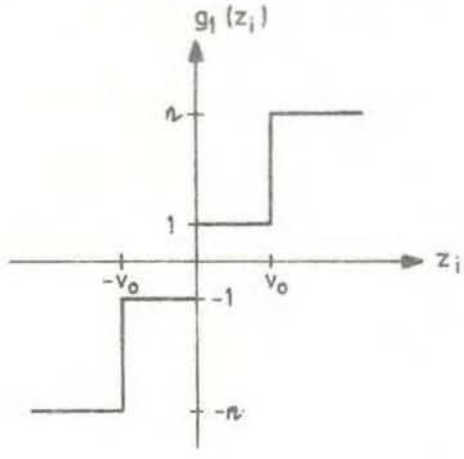

Figure 3.2. Transfer-function for 2 bits.

The autocorrelation function for Gaussian input is:

$$E[\hat{R}] = \sqrt{\frac{2}{\pi}}\sigma\rho(\tau)\left[1+(n-1)e^{-\frac{V_o^2}{2\sigma^2}}\right] \qquad (3.11)$$

and the statistical error for $\rho(\tau) << 1$ and $\frac{V_o}{\sigma} = 1.0, n = 4$ is:

$$\varepsilon_{\hat{R}} = \frac{1.07}{\sqrt{N}} \qquad (3.12)$$

$$\varepsilon_{\hat{R}} = \frac{1.04}{\sqrt{N}} \qquad \text{OVERSAMPLING}$$

The correlator is sensitive to input signal level, assuming $\sigma << V_o$ the performance is given by the hybrid correlator.

When 2 bit representation is used the multipliers can be realized by simple logic (shift-operations on the multibit sample).

MULTIBIT BY THREE-LEVEL:

The shift-operations on the multibit sample can be simplified by applying the transfer-function:

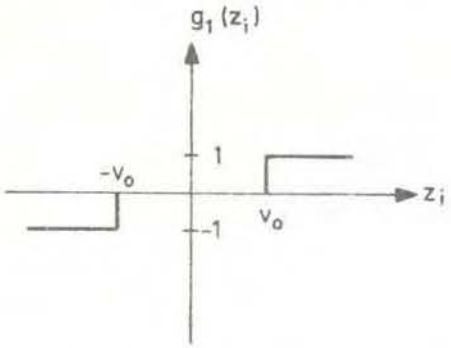

Figure 3.3. Three level quantization.

In this case:

$$E[\hat{R}] = \sqrt{\frac{2}{\pi}}\,\sigma\rho(\tau)e^{-\frac{V_o^2}{2\sigma^2}} \qquad (3.13)$$

and for the error provided $\rho(\tau) << 1$ and $\frac{V_o}{\sigma} = 0.6$:

$$\varepsilon_{\hat{R}} = \frac{1.11}{\sqrt{N}} \qquad (3.14)$$

$$\varepsilon_{\hat{R}} = \frac{1.06}{\sqrt{N}} \qquad \text{OVERSAMPLING}$$

The hardware complexity with this scheme is the same as for the hybrid correlator with additional logic functions for the non-operation of the accumulators when the delayed sample is zero.

As given, these types of correlators with the delayed samples coarse-quantized are sensitive to input signal level (σ^2), and the zero lag value doesnot vary linearly with variations of σ.

3.5. COMPARISON OF PERFORMANCE

In reference [16] integration times for different types of digital correlators are derived. In table III.2 relative integration times are given in order to obtain the same statistical accuracy as for the multibit scheme. The numbers are valid provided Gaussian input and $\rho(\tau) << 1$.

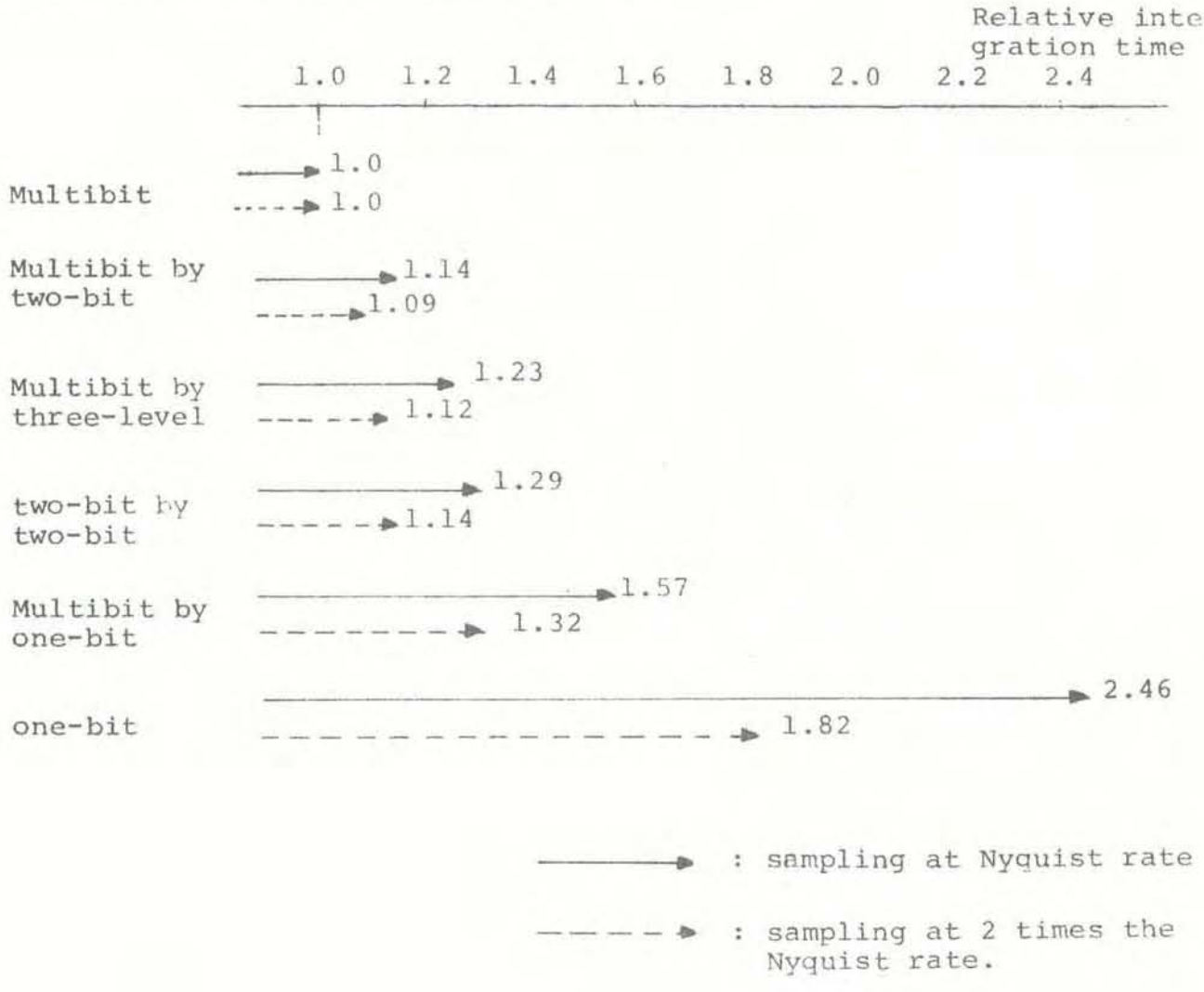

Table III.2. Comparison of integration times for different types of digital correlators.

3.6. REAL-TIME CORRELATION PERFORMED BY "SOFTWARE", REQUIREMENTS

In order to determine the requirement for the cycle-time in a CPU-orientated system the following assumptions have been made:

The system has a two-ported buffer-memory system which enables simultaneously loading of sampled data and reading samples to the CPU for computation. Two types of experiments are considered.

(α) A single-pulse experiment operating with 8 different frequencies. The repetition rate of the transmitted signal is 16.67 msec. Total number of rangegates in an interpulse period : 50. Each rangegate consists of 25 complex samples. The rangegates are overlapped.

(β) A multiple-pulse experiment (7 pulse group) operating with 8 different frequencies. The repetition rate: 10 msec. Total number of rangegates : 256.

Experiment α:

Arithmetic algorithms to be performed (M <·> denotes memory location in resultmemory):

$$\text{real part} \qquad M\langle \ell,r,1\rangle = \sum_{i=0}^{24-\ell} (X_i X_{i+\ell} + Y_i Y_{i+\ell}) + M\langle \ell,r,1\rangle$$

$$\text{imaginary part} \qquad M\langle \ell,r,2\rangle = \sum_{i=0}^{24-\ell} (X_{i+\ell} Y_i - X_i Y_{i+\ell}) + M\langle \ell,r,2\rangle \qquad (3.15)$$

$$\ell = 0,1,\ldots,24$$
$$r = 1,2,\ldots,50$$
$$x,y \text{ samples in rangegate } r$$

The same algorithm is to be performed for all 8 frequency channels. For each lag-channel (real-and-imaginary separate) and complex sample-product, the number of operations is:

2 multiplications
1 addition/subtraction
2 additions to previous content in memory (overlapped rangegates).

Assuming 49 separate lag-channels (imaginary part of zero lag not computed) the total number of operations for 25 complex samples is:

$$25 \cdot 5 + 2 \cdot 5 \cdot (24+23+....+1) = 3125$$

Half of the first and last rangegate are not overlapped. Total for the interpulse period:

$$3125 \cdot 24 + 2500 = 77500$$

Additional 4900 operations for the I/o-transfer to the memory are required. The requirement for 8 channel processing in 16.67 msec is:

659200 operations

Assuming a serial operating scheme for the system, the cycle-time is:

25.3 nsec.

In the calculations time for generating the necessary addresses to the memory is not included.

Experiment 8:

A 7 pulse group gives 21 complex lags to be computed. Assuming single products generate the estimates, the number of operations pr. rangegate is 168. For 256 gates and 8 frequencies in 10 msec, the requirement is:

430080 operations

and the cycle-time:

23.3 nsec.

The computed values show that a digital device operated in serial scheme is not realistic. Using a high-speed, bipolar micro-processor (cycle-time 300 nsec), a distributed processor - (16-20 processors) system is necessary. However, hardware multipliers have to be implemented and considerable efforts on software-, hardware-, multiport and distributed memory-systems (program and data storage) and interface-problems have to be solved.

REFERENCES

1 T. Hagfors, "EISCAT - an international project in the polar region".
Research in Norway, 1975, p. 49-54

2 J.V. Evans, "Theory and practice of ionosphere study by Thomson scatter radar".
Proc. IEEE, vol. 57, april 1969, p. 496-530

3 J.V. Evans, "High-power radar studies of the ionosphere".
Proc. IEEE, vol. 63, des. 1975, p. 1636-1650

4 P. Bauer, "Theory of waves incoherently scattered".
Phil. Trans. R. Soc., London A. 280, p. 167-191

5 EISCAT's green book, "A European incoherent scatter facility in the auroral zone, a feasibility study".
Auroral Observatory, Tromsø, Norway

6 F. du Castel and J. Testud, "Some aspects of the design concept of a European incoherent scatter facility in the auroral zone (EISCAT project)".
Radio Science, vol. 9, no. 2, feb. 1974, p. 113-119

7 R.W. Gray and D.T. Farley, "Theory of incoherent-scatter measurements using compressed pulses".
Radio Science, vol. 8, no. 2, feb. 1973, p. 123-131

8 D.T. Farley,"Multiple-pulse incoherent-scatter correlation function measurements".
Radio Science, vol. 7, no. 6, June 1972, p. 661-666

9 D.T. Farley,"Faraday rotation measurements using incoherent scatter".
Radio Science, vol. 4, no. 2, feb. 1969, p. 143-152

10 EISCAT's yellow book, "A European incoherent scatter facility in the auroral zone, UHF system and organization".

11 W. Kaufman, "Sur les correlateurs utilisant la quantification des signaux".
Report from CEPHAG, University of Grenoble.

12 B. Chabert, P. Dutang and G. Sanchez, "Correlator multibit a large bande (16 MHz)".
Laboratoire d'Electronique et de Technologie de l'Informatique, division Traitement du Signal
Report no. 1045.

13 R. Price, "A useful theorem for nonlinear devices having Gaussian Inputs".
IRE trans. on Inf. Theory, June 1958, p. 69-72.

14 J.B. Hagen, "A hybrid autocorrelator and its applications to high altitude incoherent scatter".
Thesis, National Astronomy and Ionosphere Center, NAIC 18

15 J.H. Van Vleck and D. Middleton, "The spectrum of clipped noise".
Proc. IEEE, vol. 54, no. 1, Jan. 1966, p. 2-19

16 J.B. Hagen and D.T. Farley, "Digital-correlation techniques in radio science".
Radio Science, vol. 8, no. 9, aug.-sept. 1973, p. 775-784

17 T. Hagfors, "Notes on the EISCAT data processing, various systematic effects".
Internal EISCAT note.

18 "NORD-10 input/output system".
Publ. no. ND-06.004.01 from
A/S Norsk Data-elektronikk, NORWAY

19 M.J. Baron, C. de la Beaujardiere and B. Craig, "Project 617 Radar readiness achievement program. Part a - Data processing and Analysis".
Stanford Research Institute, May 1970,
report DASA 2519-1.

20 M.J. Baron et al., "A multipulse correlator for the Chatanika radar".
Stanford Research Institute, April 1974,
report DNA 3361T

21 J. Lienard and D. Mathieu, "Correlateur destine a l'enseignement".
Report CEPHAG no. 37175, University of Grenoble.

DATA-BOOKS USED FOR HARDWARE DESIGN:

- The TTL data-book for design engineers
TEXAS INSTRUMENTS, 1973

- Supplement to the TTL data-book
TEXAS INSTRUMENTS, 1974

- The linear and interface circuits data-book
TEXAS INSTRUMENTS, 1974

- SIGNETICS data-book, 1974

- INTEL DATA CATALOG, 1975

- M6800 microcomputer, system design data
MOTOROLA, 1976

- TTL data-book, supplement no. 1 (Schottky),
FAIRCHILD, 1973

- data-sheet for K1100A(crystal clock oscillator)
MOTOROLA, 1975

- data-sheet for SEMI 1802 (1024x1-bit NMOS RAM),
EMM, 1975

MONOSTATIC INCOHERENT SCATTER OBSERVATIONS. THE IONOSPHERE AS A DISTRIBUTED, FLUCTUATIC RADAR TARGET.

In this section a one-dimensional model for the scattering is derived, i.e. the scattering volume is given in terms of altitude resolution Δh. The radar-equation is not taken into account and a plane wave notation is used for expressing the propagation as a function of altitude.

The pre-envelope of the transmitted signal can be expressed as:

$$f_T(t) = v_T(t)e^{j2\pi f_o t} \qquad (A.1)$$

$v_T(t)$: complex amplitude
f_o : radar centre frequency.

Assuming that the scattering is only occurring from an altitude h_1:

incident wave: $v_T(t-\frac{h_1}{c})e^{j2\pi f_o(t-\frac{h_1}{c})}$

c: velocity of light

backscattered wave: $N(h_1,t) \cdot v_T(t-\frac{h_1}{c})^{j2\pi f_o(t-\frac{h_1}{c})}$ (A.2)

The time-dependent function $N(h_1,t)$ is proportional to the number of electrons at altitude h_1. The backscattered signal at the receiver input is:

$$f_s(t) = N(h_1,t-\frac{h_1}{c})\ v_T(t-\frac{2h_1}{c})e^{j2\pi f_o(t-\frac{2h_1}{c})} \qquad (A.3)$$

The transmitted signal has a finite time duration and the actual backscattered signal will have contributions for a finite altitude region. The complex amplitude of the scattered signal at the receiver input can be expressed by an integral:

$$v_s(t) = \int_h a_m(h,t-\frac{h}{c})v_T(t-\frac{2h}{c})e^{-j2\pi f_o\frac{2h}{c}}\,dh \qquad (A.4)$$

where the function a_M gives the altitude and time variation of the electron density.

The autocorrelation function is defined as:

$$R_s(\tau,t) \triangleq E\left[v_s^*\ (t-\tfrac{\tau}{2})\ v_s(t+\tfrac{\tau}{2}) \right]$$

$$= \int_h \int_{h_1} E\left[a_M^*(h,t-\tfrac{\tau}{2}-\tfrac{h}{c})\ a_M(h_1,t+\tfrac{\tau}{2}-\tfrac{h_1}{c}) \right] e^{-j2\pi f_o \frac{2(h_1-h)}{c}}$$

$$\times\ v_T^*\ (t-\tfrac{\tau}{2}-\tfrac{2h}{c})\ v_T(t+\tfrac{\tau}{2}-\tfrac{2h_1}{c})\ dh_1 dh \qquad (A.5)$$

$E[\cdot]$: ensemble average

$*$: complex conjugate

Assuming the scattering process to be time stationary for h and h_1 fixed, the autocorrelation function of the density fluctuations is:

$$E\left[a_M^*(h,t-\tfrac{\tau}{2}-\tfrac{h}{c})\ a_M(h+\Delta h,t+\tfrac{\tau}{2}-\tfrac{h+\Delta h}{c}) \right] = R_M(\tau-\tfrac{\Delta h}{c},h;\Delta h) \qquad (A.6)$$

Substituting $h_1 = h+\Delta h$ in A.5:

$$R_s(\tau,t) = \int_h \int_{\Delta h} R_M(\tau-\tfrac{\Delta h}{c},h;\Delta h)\, e^{-j2\pi f_o \frac{2\Delta h}{c}}$$

$$\times\ v_T^*(t-\tfrac{\tau}{2}-\tfrac{2h}{c})\, v_T(t+\tfrac{\tau}{2}-\tfrac{2(h+\Delta h)}{c})\, d\Delta h dh \qquad (A.7)$$

The parameter Δh in R_M gives the altitude correlation of the plasma. Assuming at this point that scattering from altitudes separated by more than a Debye-length are uncorrelated, it follows:

$$R_M(\tau,h;\Delta h) \sim R_M(\tau,h;o)\,\delta(\Delta h) \qquad (A.8)$$

Performing the integration over Δh:

$$R_s(\tau,t) = \int_h R_M(\tau,h;o)\, v_T^*(t-\tfrac{\tau}{2}-\tfrac{2h}{c})\, v_T(t+\tfrac{\tau}{2}-\tfrac{2h}{c})\, dh \qquad (A.9)$$

The signal at the receiver input is non-stationary in time, the time dependence expresses the altitude discrimination. The altitude resolution is determined by the transmitted waveform. The altitude weight-function is:

$$W_T(\tau,h;t) \triangleq v_T^*(t-\frac{\tau}{2}-\frac{2h}{c})v_T(t+\frac{\tau}{2}-\frac{2h}{c}) \qquad (A.10)$$

Then:

$$R_S(\tau,t) = \int_h R_M(\tau,h)W_T(\tau,h;t)dh \qquad (A.11)$$

The paramter $\Delta h=0$ in A.9 is dropped for simplicity. The information one wishes to extract, is R_M as a function of τ and h. Caused by the linear operation of R_M with W_T, variations on R_M with h are indistinguishable from τ-variations. By the assumption that R_M is constant over h on a scale given by W_T and:

$$v_T(t) = \begin{cases} \neq 0 & \text{for } |t| \leq \frac{\tau_T}{2} \\ = 0 & \text{else} \end{cases} \qquad (A.12)$$

the autocorrelation function at the receiver input is:

$$R_S(\tau,t) = \begin{cases} R_M(\tau,h=\frac{ct}{2}) \times R_T(\tau;t) & |\tau| \leq \tau_T \\ 0 & |\tau| > \tau_T \end{cases} \qquad (A.13)$$

where

$$R_T(\tau;t) \triangleq \int_{\frac{1}{2}(ct-\Delta h)}^{\frac{1}{2}(ct+\Delta h)} W_T(\tau,\frac{ct}{2};t)dh \ , \ \Delta h=\frac{c}{2}(\tau_T-\tau) \qquad (A.14)$$

The receiver system can be described by an impulse-response $h_R(t)$ (pre-envelope), and the signal at the IF output is given by the convolution integral:

$$f_o(t) = \int_\theta f_s(t-\theta)h_R(\theta)d\theta \qquad (A.15)$$

By the introduction of the complex amplitude through:

$$h_{R,LP}(\theta) = h_R(\theta)e^{-j2\pi f_o\theta} \tag{A.16}$$

the autocorrelation function of the observed signal (for the complex amplitude) is:

$$R_o(\tau,t) \triangleq E\left[v_o^*(t-\tfrac{\tau}{2})\, v_o(t+\tfrac{\tau}{2})\right]$$

$$= \int_{\theta}\int_{\theta_1} R_s(\tau+\theta-\theta_1,\ t-\tfrac{\theta+\theta_1}{2})h^*_{R,LP}(\theta)h_{R,LP}(\theta_1)d\theta_1 d\theta$$

$$R_o(\tau,t) = \int_{\theta}\int_{\theta_1}\int_{h} R_M(\tau+\theta-\theta_1,h)W_T(\tau+\theta-\theta_1,\ h;t-\tfrac{\theta+\theta_1}{2})$$

$$\times\ h^*_{R,LP}(\theta)h_{R,LP}(\theta_1)dh d\theta_1 d\theta$$

By the substitution: $\theta_1 = \theta+\alpha$

$$R_o(\tau,t) = \int_{\theta}\int_{\alpha}\int_{h} R_M(\tau-\alpha,h)W_T(\tau-\alpha,h;t-\theta-\tfrac{\alpha}{2})$$

$$\times\ h^*_{R,LP}(\theta)h_{R,LP}(\theta+\alpha)dh d\alpha d\theta$$

Following the same argumentation as above assuming R_M to be constant over the actual altitude interval:

$$R_o(\tau,t) = \int_\alpha R_M(\tau-\alpha,h)\left[\int_h W_T(\tau-\alpha,h;t)\,dh\right] \cdot \left[\int_\theta h^*_{R,LP}(\theta)\,h_{R,LP}(\theta+\alpha)\,d\theta\right]d\alpha$$

Then, by definition of the receiver system's "autocorrelation function".

$$R_R(\alpha) \triangleq \int_\theta h^*_{R,LP}(\theta)\,h_{R,LP}(\theta+\alpha)\,d\theta \qquad (A.17)$$

the autocorrelation function of the observed signal is:

$$R_o(\tau,t) = \int_\alpha R_M(\tau-\alpha,h)\,R_T(\tau-\alpha;t)\cdot R_R(\alpha)\,d\alpha$$

$$= \left[\, R_M \times R_T \,\right] \circledast R_R \qquad (A.18)$$

$\circledast$ convolution

In order to determine the validity of the approximation given in eq. A.8, the function $R_s(\tau,t)$ in A.7 can be expressed as:

$$R_s(\tau,t) = \int_h \int_{\Delta h} \int_f W_M(f,h;\Delta h)\, e^{-j2\pi\left(\frac{2f_0}{c}+\frac{f}{c}\right)\Delta h}\, e^{j2\pi f\tau}$$

$$\times\, v^*_T\left(t-\tfrac{\tau}{2}-\tfrac{2h}{c}\right) v_T\left(t+\tfrac{\tau}{2}-\tfrac{2(h+\Delta h)}{c}\right) df\,d\Delta h\,dh \qquad (A.19)$$

where the density fluctuation spectrum is defined by:

$$W_M(f,h;\Delta h) \triangleq \mathcal{F}\left\{R_M(\tau,h;\Delta h)\right\} \qquad (A.20)$$

The Fouriertransform of the last term in A.19 is:

$$\mathcal{F}\{v_T(t + \frac{\tau}{2} - \frac{2(h+\Delta h)}{c})\} = V_T(f)e^{-j2\pi f(\frac{2(h+\Delta h)}{c} - \frac{\tau}{2})} \qquad (A.21)$$

Assuming the spectrum W_M is constant over the actual altitude-interval, eq. A.19 can be rewritten with the substitution in A.21:

$$R_s(\tau,t) = \int_{f'} V_T(f')e^{j2\pi f'\tau}\Big[\int_h v_T^*(t - \frac{\tau}{2} - \frac{2h}{c})e^{j2\pi f'(t-\frac{\tau}{2}-\frac{2h}{c})}\Big]$$

$$\times \Big[\int_f e^{j2\pi f\tau}\int_{\Delta h} W_M(f,h,\Delta h)e^{-j2\pi(\frac{2(f_0+f')}{c} + \frac{f}{c})\Delta h}\, d\Delta h\, df\Big]\Big)df'$$

$$= \frac{c}{2}\int_{f'}|V_T(f')|^2 e^{j2\pi f'\tau}\Big[\int_f e^{j2\pi f\tau}\int_{\Delta h} W_M(f,h,\Delta h)$$

$$\cdot e^{-j2\pi(\frac{2(f_0+f')}{c} + \frac{f}{c})\Delta h}\, d\Delta h\, df\Big]\, df'$$

The integral over Δh represents a spatial Fouriertransform:

$$\int_{\Delta h} W_M(f,h,\Delta h)e^{-jk\Delta h}d\Delta h \triangleq W_M(f,h,k) \qquad (A.22)$$

$$R_s(\tau,t) = \frac{c}{2}\int_{f'}|V_T(f')|^2 e^{j2\pi f'\tau}\Big[\int_f W_M(f,h,\frac{4\pi(f_0+f')}{c} + \frac{2\pi f}{c})$$

$$\cdot e^{j2\pi f\tau}df\Big]df' \qquad (A.23)$$

Refining now an autocorrelation function of the spatial fluctuation spectrum:

$$R_{M,k}(\tau,h,2k_T) \triangleq \int_f W_M(f,\ h,\ 2k_T + \frac{2\pi f}{c})e^{j2\pi f}\, df \qquad (A.24)$$

it follows:

$$R_s(\tau,t) = \frac{c}{2} \int_{f'} |V_T(f')|^2 e^{j2\pi f'\tau} R_{M,k}(\tau,h,\ 2k_{TO} + \frac{4\pi f'}{c}) df' \quad (A.25)$$

Provided the autocorrelation function $R_{M,k}$ is constant in the integration over f':

$$R_s(\tau,t) = R_{M,k}(\tau,h,2k_{TO}) \frac{c}{2} \int_{f'} |V_T(f')|^2 e^{j2\pi f'\tau} df' \quad (A.26)$$

or by introducing the autocorrelation function of the transmitted signal (eq. A.14):

$$R_s(\tau,t) = R_{M,k}(\tau,h,2k_{TO}) \cdot R_T(\tau,t) \quad (A.27)$$

$$k_{TO} = \frac{2\pi f_0}{c} \ , \ f_0: \text{ radar centre frequency}$$

Eq. A.27 gives that the plasma autocorrelation function to be estimated is defined by the inverse transform of the plasma spatial fluctuation spectrum (eq. A.24) and that the autocorrelation function for the plasma and the transmitted signal can only be separated provided

- the plasma autocorrelation function is assumed constant over the altitude-interval determined by the transmitted signal,
- the plasma autocorrelation function is assumed constant for wavenumbers

$$2k_{TO} + \frac{4\pi f'}{c}$$

where f' can vary over a frequency-band determined by the spectrum of the transmitted signal.

With the approximation in eq. A.8 all frequency variations on R_M have been neglected. As stated in eq. A.25, however, the actual autocorrelation function is given by a weighted sum of autocorrelation functions of the spatial fluctuation spectrum which have a correct scale for backscattering.

EISCAT TRANSMITTER SYSTEM CHARACTERISTICS.

UHF-SYSTEM

Centre frequencies	: 933.5 ± 5 MHz 11 frequencies can be selected from 931 MHz to 936 MHz in steps of 500 kHz.
Peak power output$_{MAX}$	: 2 MW
Average power$_{MAX}$	: 250 kW
Duty cycle	: 0-12.5% variable
Pulse rep. rate	: 0-1 kHz variable
Pulse length	: 10 μsec - 10 msec variable
Modulation	: Pulsed, with facilities for 180 phase-modulation and frequency-hop within the pulse or from pulse to pulse. A multipulse mode giving groups of from 2 to 10 pulses.

VHF-SYSTEM

Centre frequencies	: 224 ± 1.5 MHz 11 frequencies from 222.75 to 225.25 MHz in steps of 250 kHz.
Peak power output$_{MAX}$	: 5 MW
Average power$_{MAX}$	: 625 kW
Duty cycle	: 0-12.5% variable
Pulse rep. rate	: 0-1 kHz variable
Pulse length	: 10 μsec - 1 msec variable
Modulation	: Pulsed, with facilities for 180^0 phase-modulation and frequency-hop. Multipulse mode with 2 to 10 pulses. Flip between right- and left-circular polarization transmitted are controlled in real-time.

EISCAT SCIENTIFIC ASSOCIATION
S-981 01 KIRUNA 1, SWEDEN
TELEPHONE 0980/187 40
TELEX 8754 GEOFYSK S